Title:	*Receiver Design Tools*
Author:	AM1 LLC
Abstract:	This memo summarizes a number of results which are very helpful in receiver design.
Disclaimer:	*The technical information and opinions provided in this document are believed to be accurate, but no warranty, assurance, or indemnification of any kind is granted nor implied as to the completeness, accuracy, or suitability of this information for any purpose whatsoever. Upon receipt of this information or any derivatives of it, receiving party acknowledges that this information may contain inaccuracies or errors, and AM1 expressly excludes any liability for any such inaccuracies or errors to the fullest extent permitted by law. AM1 assumes no liability whatsoever for any damages or losses resulting from the use or reliance upon the information contained or absent herein.* *Furthermore, AM1 provides no warranty, assurance, or indemnification of any kind in regard to the possible infringement of the provided material upon the intellectual property rights of others. AM1 assumes no liability of any kind concerning such property rights. Upon receipt of this information or any derivatives of it, receiving party acknowledges that this information may possibly infringe upon the intellectual property rights of others, and is itself solely responsible for the proper use of the information and opinions contained herein.*
Date:	25 Jan 2018
Version:	1.0

1 Receiver Noise Figure

Computation of the cascaded receiver noise figure is probably one of the best known receiver design formula. All of the calculations are done in terms of power. The use of receiver *noise figure* and *noise factor* come up in this context where

$$NoiseFigure_{dB} = 10\log_{10}\left(NoiseFactor\right) \tag{1}$$

where *NoiseFactor* is the numerical ratio of a stage output noise (spectral density) to input noise (spectral density).

For two blocks in cascade as shown in Figure 1, the input-referred *noise factor* is given by

$$NF = F_1 + \frac{F_2 - 1}{G_1} = \frac{F_1 G_1 + F_2 - 1}{G_1} \tag{2}$$

and the corresponding noise figure is given by [3]

$$NFig_{dB} = 10\log_{10}\left(F_1\right) + 10\log_{10}\left(1 + \frac{F_2 - 1}{F_1 G_1}\right) \text{ dB} \tag{3}$$

This form is convenient for working right-to-left in Figure 2 and computing the cascaded noise figure. For a cascade of *N* blocks as shown in Figure 2, the resultant input-referred *noise factor* can also be found as

$$NF = F_1 + \sum_{k=2}^{N}\left[\frac{F_k - 1}{\left(\prod_{j=1}^{k-1} G_j\right)}\right] \tag{4}$$

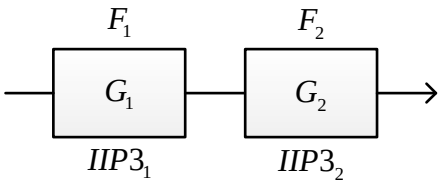

Figure 1 Cascade of two receiver blocks left-to-right. The F_k are *noise factors*, the G_k values are numeric stage power-gains, and the $IIP3_k$ are individual block input 3rd-order intercept points.

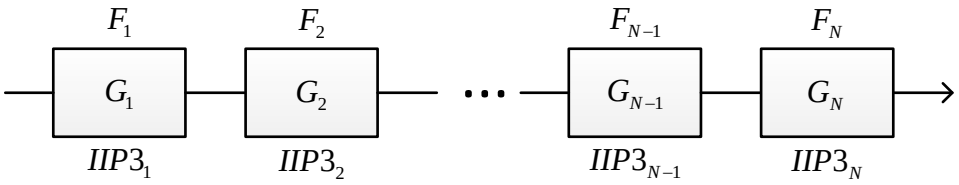

Figure 2 Cascade of *N* blocks using the same notation as in Figure 1

2 Intercept Points

2.1 3rd-Order Intercept Point With Single Input Tone

The single-tone case will be considered first where the output voltage for a block is represented by a memoryless nonlinearity given by [6]

$$e_o = k_1 e_i + k_2 e_i^2 + k_3 e_i^3 + \ldots \tag{5}$$

Taking $e_i = A\cos(\omega_1 t)$, e_o can be written as

$$e_o = \frac{1}{2}k_2 A^2 + \left(k_1 A + \frac{3}{4}k_3 A^3\right)\cos(\omega_1 t) + \frac{1}{2}k_2 A^2 \cos(2\omega_1 t) + \frac{1}{4}k_3 A^3 \cos(3\omega_1 t) \tag{6}$$

The gain at the fundamental frequency is given by

$$G = 20\log_{10}\left(k_1 + \frac{3}{4}k_3 A^2\right)\ \text{dB} \tag{7}$$

compared to the linear gain defined as

$$G_0 = 20\log_{10}(k_1)\ \text{dB} \tag{8}$$

The –1 dB compression point is defined as the input power level at which $G - G_0 = -1\ \text{dB}$. This occurs for

$$k_1 + \frac{3}{4}k_3 A^2 = 0.891 k_1 \tag{9}$$

which leads to

$$A^2 = 0.145\left|\frac{k_1}{k_3}\right| \text{ for } k_3 < 0 \tag{10}$$

Assuming that the system is operating at 50Ω, it can be shown that the output 1 dB compression point is given by

$$P_{1dB} = 10\log_{10}\left(\frac{k_1^3}{|k_3|}\right) + 0.62 \text{ dBm for } R_o = 50\Omega \tag{11}$$

2.2 3rd-Order Intercept Point With Two Input Tones

In the case of a two-tone input given by

$$e_i = A\left[\cos(\omega_1 t) + \cos(\omega_2 t)\right] \tag{12}$$

the output voltage is given by [6]

$$\begin{aligned} e_o = {} & k_2A^2 + \left(k_1A + \frac{9}{4}k_3A^3\right)\cos(\omega_1 t) + \left(k_1A + \frac{9}{4}k_3A^3\right)\cos(\omega_2 t) + \\ & k_2A^2\cos\left[(\omega_1 - \omega_2)t\right] + k_2A^2\cos\left[(\omega_1 + \omega_2)t\right] + \frac{1}{2}k_2A^2\cos(2\omega_1 t) + \frac{1}{2}k_2A^2\cos(2\omega_2 t) + \\ & \frac{3}{4}k_3A^3\cos\left[(2\omega_1 - \omega_2)t\right] + \frac{3}{4}k_3A^3\cos\left[(2\omega_2 - \omega_1)t\right] + \\ & \frac{3}{4}k_3A^3\cos\left[(2\omega_1 + \omega_2)t\right] + \frac{3}{4}k_3A^3\cos\left[(2\omega_2 + \omega_1)t\right] + \frac{1}{4}k_3A^3\cos(3\omega_1 t) + \frac{1}{4}k_3A^3\cos(3\omega_2 t) \end{aligned} \tag{13}$$

The input 3rd-order intercept point is defined as the input power level of each tone at which the output power at any one of the intermodulation frequencies, e.g., $P_{(2\omega_1-\omega_2)}$, equals the output power at the desired frequency ω_1 given by P_o as if the low-level input was conveyed to the output in a completely linear manner (i.e., voltage-gain = k_1). From (13), the output power level for the desired tone at frequency ω_1 when the two-port is linear is given by

$$P_o = 10\log_{10}\left[\left(\frac{k_1A}{\sqrt{2}}\right)^2\frac{10^3}{R_o}\right] \text{ dBm} \tag{14}$$

where $R_o = 50\Omega$ is generally assumed. The output power level for the tone at ω_1 including the nonlinearities is given by

$$P_{\omega_1} = 10\log\left[\left(\frac{k_1A + \frac{9}{4}k_3A^3}{\sqrt{2}}\right)^2\frac{10^3}{R_o}\right] \text{ dBm} \tag{15}$$

The output power for each of the intermodulation frequencies is given by

$$P_{(2\omega_1-\omega_2)} = 10\log_{10}\left[\left(\frac{\frac{3}{4}k_3A^3}{\sqrt{2}}\right)^2\frac{10^3}{R_o}\right]\ \text{dBm} \tag{16}$$

At the intercept point $P_{(2\omega_1-\omega_2)} = P_o$ which leads from (14) and (16) to

$$k_1A = \frac{3}{4}k_3A^3 \tag{17}$$

and finally

$$A^2\left(\text{at intercept point}\right) = \frac{4}{3}\left|\frac{k_1}{k_3}\right| \tag{18}$$

Consequently, the input power level of <u>each</u> input tone corresponding to the 3rd-order input intercept point is given by

$$\begin{aligned} P_{input\_each\_tone} &= 10\log_{10}\left[\frac{A^2}{2}\frac{10^3}{R_o}\right]\ \text{dBm} \\ &= 10\log_{10}\left(\frac{2}{3}\left|\frac{k_1}{k_3}\right|\frac{10^3}{R_o}\right)\ \text{dBm} \\ &= 10\log_{10}\left(\left|\frac{k_1}{k_3}\right|\right) + 11.25 \quad \text{dBm for } R_o = 50\Omega \end{aligned} \tag{19}$$

The <u>input</u> 3rd-order intercept point is therefore given by the single-tone input power value $P_{input\_each\_tone}$.

The <u>output</u> 3rd-order intercept point is similarly given by

$$\begin{aligned} P_o &= 10\log_{10}\left[k_1^2\frac{A^2}{2}\frac{10^3}{R_o}\right]\ \text{dBm} \\ &= 10\log_{10}\left(\frac{2}{3}\left|\frac{k_1^3}{k_3}\right|\frac{10^3}{R_o}\right)\ \text{dBm} \\ &= 10\log_{10}\left(\left|\frac{k_1^3}{k_3}\right|\right) + 11.25 \quad \text{dBm for } R_o = 50\Omega \end{aligned} \tag{20}$$

As a side-note, the solution for A^2 corresponding to $P_{(2\omega_1-\omega_2)} = P_{\omega_1}$ from (15) and (16) is given by

$$\frac{3}{4}k_3A^3 = k_1A + \frac{9}{4}k_3A^3 \tag{21}$$

which ultimately produces $A^2 = \frac{2}{3}\left|\frac{k_1}{k_3}\right|$ and a corresponding single-tone input power level corresponding to this *pseudo* intercept point of

$$\begin{aligned} P'_{input\_each\_tone} &= 10\log_{10}\left[\frac{1}{3}\left|\frac{k_1}{k_3}\right|\frac{10^3}{R_o}\right] \text{ dBm} \\ &= 10\log_{10}\left(\left|\frac{k_1}{k_3}\right|\right) + 8.24 \text{ dBm} \\ &= P_{input\_each\_tone} - 3.01 \text{ dBm} \end{aligned} \tag{22}$$

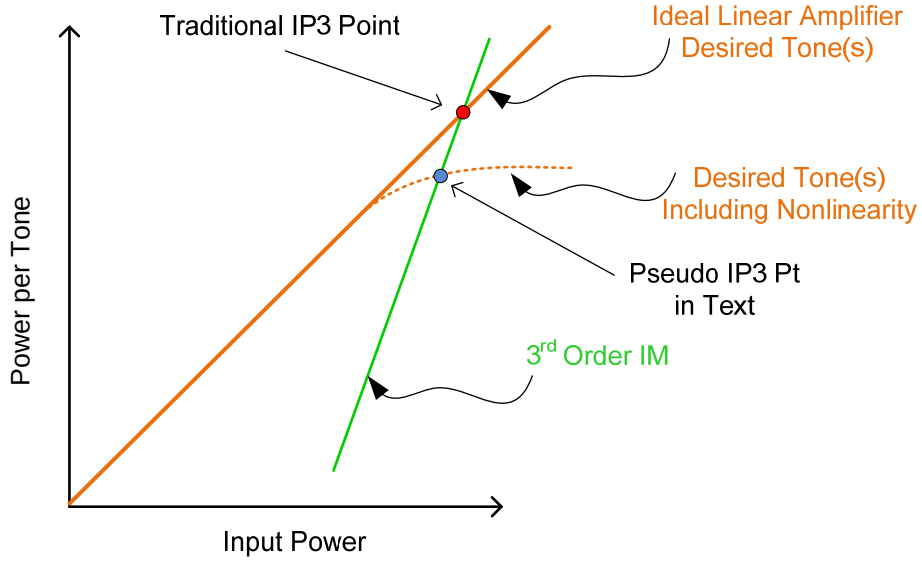

Figure 3 Traditional input IP3 point defined per (19) and pseudo-IP3 point defined per (22)

Continuing from (16), the output power level at $2\omega_1 - \omega_2$ can also be written as

$$\begin{aligned} P_{(2\omega_1-\omega_2)} &= 10\log_{10}\left[\left(\frac{\frac{3}{4}k_3A^3}{\sqrt{2}}\right)^2\frac{10^3}{R_o}\right] \text{ dBm} \\ &= 10\log_{10}\left[\frac{9}{32}k_3^2A^6\frac{10^3}{R_o}\right] \\ &= 10\log_{10}\left(A^6\right) + 10\log_{10}\left(\frac{9}{32}k_3^2\frac{10^3}{R_o}\right) \end{aligned} \tag{23}$$

Note that from (14),

$$\begin{aligned} 3P_o &= 10\log_{10}\left[\left(\frac{k_1 A}{\sqrt{2}}\right)^6\left(\frac{10^3}{R_o}\right)^3\right] \\ &= 10\log_{10}\left(A^6\right)+10\log_{10}\left[\frac{k_1^6}{8}\left(\frac{10^3}{R_o}\right)^3\right] \end{aligned} \tag{24}$$

Solving for $10\log_{10}\left(A^6\right)$ in (24) and substituting into (23) produces

$$\begin{aligned} P_{(2\omega_1-\omega_2)} &= 3P_o - 10\log_{10}\left[\frac{k_1^6}{8}\left(\frac{10^3}{R_o}\right)^3\right]+10\log_{10}\left(\frac{9}{32}k_3^2\frac{10^3}{R_o}\right) \\ &= 3P_o - 10\log_{10}\left[\frac{k_1^6}{8}\left(\frac{10^3}{R_o}\right)^3\frac{32}{9}\frac{1}{k_3^2}\left(\frac{R_o}{10^3}\right)\right] \\ &= 3P_o - 10\log_{10}\left[\frac{4}{9}\left|\frac{k_1^3}{k_3}\right|^2\left(\frac{10^3}{R_o}\right)^2\right] \\ &= 3P_o - 2P_{output\_one\_tone\_\omega_1} \\ &= 3P_o - 2\,OIP3 \end{aligned} \tag{25}$$

It is a simple matter to refer all of the previous calculations back to the input of the block thereby resulting in

$$P_{(2\omega_1-\omega_2)\text{ referred to Input}} = 3P_i - 2\,IIP3 \tag{26}$$

Reiterating then, the intercept points correspond to the single-tone power level at which an individual intermodulation product has the same power level as one of the desired tones had no nonlinearities been present. Specifically,

$$\begin{aligned} IIP3 &= 10\log_{10}\left(\frac{2}{3}\left|\frac{k_1}{k_3}\right|\frac{10^3}{R_o}\right)\ \text{dBm} \\ &= 10\log_{10}\left(\left|\frac{k_1}{k_3}\right|\right)+11.25\ \text{dBm for } R_o = 50\Omega \end{aligned} \tag{27}$$

$$\begin{aligned} OIP3 &= 10\log_{10}\left(\frac{2}{3}\left|\frac{k_1^3}{k_3}\right|\frac{10^3}{R_o}\right)\ \text{dBm} \\ &= 10\log_{10}\left(\left|\frac{k_1^3}{k_3}\right|\right)+11.25\ \text{dBm for } R_o = 50\Omega \end{aligned} \tag{28}$$

Referring back to (11), the output 1 dB compression point and output 3rd-order intercept point are related as

$$OIP3 = P_{1dB} + 10.63\ \text{dBm for } R_o = 50\Omega \tag{29}$$

2.3 2nd-Order Intercept Point

Calculations similar to those performed in the previous section §2.1 can be applied to the 2nd-order case as well. From (13) the potentially troublesome 2nd-order intermodulation term at frequency $(\omega_1 - \omega_2)$ exhibits an output power level of

$$P_{(\omega_1-\omega_2)} = 10\log_{10}\left[\left(\frac{k_2 A^2}{\sqrt{2}}\right)^2 \frac{10^3}{R_o}\right] \text{ dBm} \tag{30}$$

At the 2nd-order intercept point, $P_{(\omega_1-\omega_2)} = P_o$ where P_o is still given by (14). The solution is given by $A = \left|\frac{k_1}{k_2}\right|$. The output– and input–referred 2nd-order intercept points are then given by

$$OIP2 = 10\log_{10}\left[\frac{1}{2}\frac{k_1^4}{k_2^2}\frac{10}{R_o}\right] \text{ dBm} \tag{31}$$

$$IIP2 = 10\log_{10}\left[\frac{1}{2}\left|\frac{k_1}{k_2}\right|^2 \frac{10^3}{R_o}\right] \text{ dBm} \tag{32}$$

2.4 Cascaded 3rd-Order Intercept Point

Assuming that a cascade of blocks is to be considered as shown in Figure 2 where the input and output impedance of each block is R_o (typically 50Ω), the input intercept point for the cascade is given by

$$IIP3 = \left[\sum_{k=1}^{N}\left(\frac{\prod_{j=0}^{k-1} G_j}{IIP3_k}\right)\right]^{-1} \tag{33}$$

where all of the block parameters are numeric in nature and G_0 = 1.0. The input 3rd-order intercept point for the k^{th} block is given by $IIP3_k$ whereas the power-gain for the k^{th} block is represented by G_k. In the simplified case where two blocks are cascaded left-to-right as shown in Figure 1, the input intercept point is given by

$$IIP3 = \left[\frac{1}{IIP3_1} + \frac{G_1}{IIP3_2}\right]^{-1} \tag{34}$$

This latter formula may be applied recursively from right-to-left if this simplifies the analysis.

2.5 Filters Present with 3rd-Order Intercept Point

When filters are present in the cascade, the receiver's *IIP3* is also a function of the frequency offset used for the two input tones. It can be shown [4] that the filters can be modeled as frequency-independent networks for each value of tone frequency separation Δf using a constant-loss attenuator pad at each filter location whose insertion loss is

$$L_{pad} = \frac{L_{fil}(\Delta f)\sqrt{L_{fil}(2\Delta f)}}{\sqrt{L_{fil}(0)}} \tag{35}$$

where $L_{fil}(f)$ is the filter's numerical insertion loss at frequency separation *f* from the filter's center frequency. In decibel form, (35) can be rewritten as

$$\begin{aligned} L_{pad}(dB) &= L_{fil}(\Delta f)_{dB} + \frac{1}{2}L_{fil}(2\Delta f)_{dB} - \frac{1}{2}L_{fil}(0)_{dB} \\ &= L_{fil}(0)_{dB} + \left[L_{fil}(\Delta f)_{dB} - L_{fil}(0)_{dB}\right] + \frac{1}{2}\left[L_{fil}(2\Delta f)_{dB} - L_{fil}(0)_{dB}\right] \\ &= L_{fil}(0)_{dB} + R(\Delta f) + \frac{1}{2}R(2\Delta f) \end{aligned} \tag{36}$$

where

$$R(f) = 10\log_{10}\left[\frac{L_{fil}(f)}{L_{fil}(0)}\right] \tag{37}$$

which is the relative stopband loss at frequency *f* compared to the insertion loss of the filter at its center frequency.

2.6 3rd-Order Output Intercept Point

Similarly, the *output 3rd-order intercept point* for the complete cascade is given by

$$OIP3 = \left[\sum_{k=1}^{N}\frac{1}{OIP3_k\left(\prod_{j=k+1}^{N}G_j\right)}\right]^{-1} \tag{38}$$

where the *output 3rd-order intercept* of the j^{th} block is given by $OIP3_j$. In the simplified case where two blocks are cascaded as shown in Figure 1, the output intercept point is given by

$$OIP3 = \left[\frac{1}{OIP3_1 G_2} + \frac{1}{OIP3_2}\right]^{-1} \tag{39}$$

3 3rd-Order (Instantaneous) Dynamic Range

Given an input intercept point $IIP3_{dBm}$, the resultant intermodulation product has a level of

$$\begin{aligned} IM_{dBm} &= IIP3_{dBm} - 3\left(IIP3_{dBm} - P_{tone}\right) \\ &= -2IIP3_{dBm} + 3P_{tone} \end{aligned} \tag{40}$$

where P_{tone} is the input power level of each individual tone in dBm. Denoting the receiver's *minimum detectable signal* as MDS_{dBm}, the input tone power at which the intermodulation products equal the minimum detectable signal is

$$P_{tone\_MDS} = \frac{2IIP3_{dBm} + MDS_{dBm}}{3} \tag{41}$$

The difference between this input signal level (at which the intermodulation products equal the minimum detectable signal level) and the minimum detectable signal is what is known as the *3rd-order instantaneous dynamic range*, DR_{dB}. Mathematically,

$$\begin{aligned} DR_{dB} &= P_{tone\_MDS} - MDS \\ &= \frac{2IIP3_{dBm} + MDS_{dBm}}{3} - MDS_{dBm} = \frac{2}{3}\left(IIP3_{dBm} - MDS_{dBm}\right) \end{aligned} \tag{42}$$

4 Receiver Blocking

Even if a strong unwanted signal does not create on-channel intermodulation products, it can lead to desensitization of the receiver simply due to saturation in the receive chain. In the present context, receiver blocking *does not* include any degradation due to reciprocal mixing which is discussed later in §8.

Receiver blocking is often specified as the out-of-band signal level which degrades the receiver's sensitivity by 3 dB [7]. While this much degradation may be tolerable for terrestrial communications, this may be unacceptable for disadvantaged satellite communications. In the context of GSM, the blocking test is performed as follows [7]:

> *The blocking test for GSM is performed by applying a GMSK modulated desired signal 3 dB above the required receiver reference sensitivity. Then a single unmodulated tone (simple sinewave) is applied to the receiver at discrete increments of 200 kHz from the desired signal with a magnitude as given by the blocking requirements of GSM, E-GSM, DCS1800, and PCS1900.*

Receiver blocking requirements for E-GSM are shown in Figure 4 below. This specification does not differentiate between the different blocking mechanisms but is rather a "black-box" overall performance requirement. Representative receiver quantities for different cell phone standards are also provided in Figure 5 for additional context.

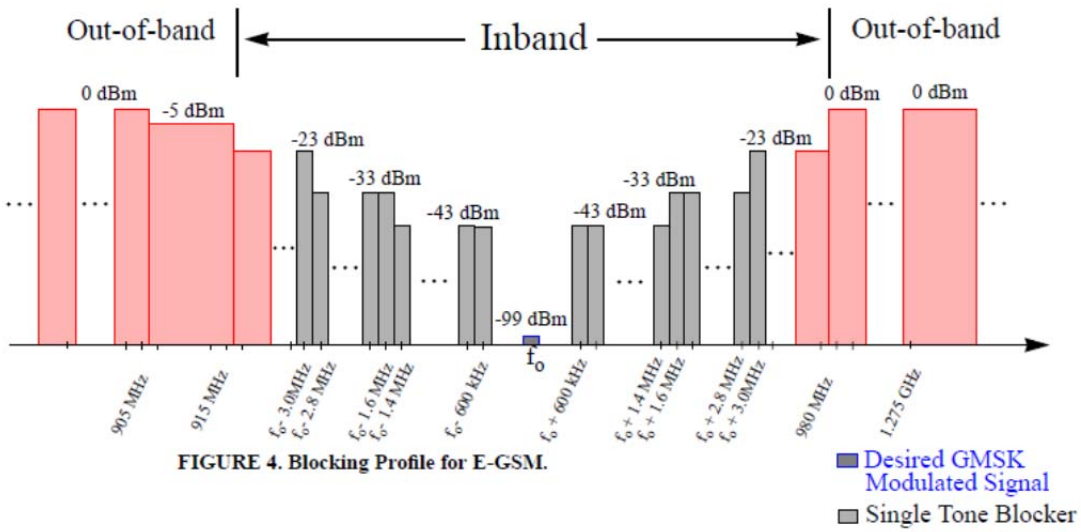

Figure 4 Receiver blocking requirements for E-GSM [7]

Standard	Sensitivity (dBm)	Input Noise (dBm)	Input SNR (dB)	Required C/N (dB)	Required NF (dB)
GSM	-102	-120.8	18.8	9	9.8
E-GSM	-102	-120.8	18.8	9	9.8
DCS1800	-100	-120.8	20.8	9	11.8
PCS 1900	-102	-120.8	18.8	9	9.8
DECT	-83	-112.3	29.3	10.3	19.0
GPS	-130	-110.9	-19.0	N/A	14

Figure 5 Typical commercial standard requirements [7]

Blocking-related receiver desensitization primarily occurs due to (i) reduced stage-gain which translates into poorer noise figure performance per (4) and (ii) increased noise figure of individual receiver stages due to the high signal level present. As noted above, the blocking test is normally done with an unmodulated sinusoidal carrier. Otherwise, cross-modulation between the desired and blocking signals occurs which further degrades the effective sensitivity of the receiver as discussed in §5.

To continue, assume that the input signal is given by

$$e_i = I\cos(\omega_1 t) - Q\sin(\omega_1 t) + A\cos(\omega_2 t) \tag{43}$$

Assume that the same type of memoryless nonlinearity given by (5) is in play. A lot of pesky trigonometry is needed to compute e_i^2 and e_i^3. For the first item,

$$\begin{aligned} e_i^2 = {} & \frac{I^2+Q^2+A^2}{2} + \left(\frac{I^2-Q^2}{2}\right)\cos(2\omega_1 t) + \frac{A^2}{2}\cos(2\omega_2 t) - IQ\sin(2\omega_1 t) + \\ & IA\cos\left[(\omega_1+\omega_2)t\right] + IA\cos\left[(\omega_1-\omega_2)t\right] - QA\sin\left[(\omega_1-\omega_2)t\right] - QA\sin\left[(\omega_1+\omega_2)t\right] \end{aligned} \tag{44}$$

In subsequent equations, the explicit dependence on *t* will be omitted for brevity.

As shown by (44), there are no signal terms that fall near the desired signal at ω_1 unless ω_2 is approximately equal to the second harmonic of ω_1. This should not occur in most receiver designs

because preselection filtering should knock down any signal energy near this second harmonic region. One notable exception is, however, for input frequencies less than a given limit where preselection filtering is impractical and harmonic-rejection mixing can be used to assist with this deficiency. A similar situation occurs when ω_2 is a sub-harmonic of ω_1. The second-order terms of greatest consequence from (44) are[1]:

DC terms in the context of Direct-Conversion:

$$\frac{I^2+Q^2+A^2}{2} \tag{45}$$

Strong interferer near half-frequency of desired:

$$\frac{A^2}{2}\cos\left(2\omega_2 t\right) \tag{46}$$

Strong interferer near 2nd harmonic of desired:

$$IA\cos\left[\left(\omega_1-\omega_2\right)t\right]-QA\sin\left[\left(\omega_1-\omega_2\right)t\right] \tag{47}$$

The most damaging term in the context of receiver blocking when it comes to direct-conversion receivers is (45) primarily because it is entirely independent of the blocker's frequency. In contrast, the superheterodyne structure is largely free of 2nd-order linearity issues except for the specific frequency cases identified in (46) and (47).

The number of terms involved with computing e_i^3 is quite laborious so the results are organized in tabular form in Table 1. The most onerous terms when it comes to the strong blocking signal are in the first two rows of the table.

Table 1 3rd-Order Terms

Term	*Frequency Term*	*Amplitude*	*Comments*
1	$\cos\left(\omega_1 t\right)$	$\frac{3}{4}I^3+\frac{3}{4}IQ^2+\frac{3}{4}IA^2$	On Channel
2	$\sin\left(\omega_1 t\right)$	$-\frac{3}{4}Q^3-\frac{3}{4}QI^2-\frac{3}{2}QA^2$	On Channel
3	$\cos\left[\left(2\omega_1-\omega_2\right)t\right]$	$\frac{3}{4}A\left(I^2-Q^2\right)$	Intermodulation
4	$\sin\left[\left(2\omega_1-\omega_2\right)t\right]$	$-\frac{3}{2}IQA$	Intermodulation
5	$\cos\left[\left(2\omega_2-\omega_1\right)t\right]$	$\frac{3}{4}IA^2$	Intermodulation
6	$\sin\left[\left(2\omega_2-\omega_1\right)t\right]$	$\frac{3}{4}QA^2$	Intermodulation
7	$\cos\left(\omega_2 t\right)$	$\frac{3}{4}A^3+\frac{3}{2}A\left(I^2+Q^2\right)$	–

[1] Verified in U22178_Cross_Modulation.mcd.

Term	Frequency Term	Amplitude	Comments
8	$\cos(3\omega_1 t)$	$\frac{I^3}{4}-\frac{3}{4}IQ^2$	–
9	$\sin(3\omega_1 t)$	$\frac{Q^3}{4}-\frac{3}{4}I^2Q$	–
10	$\cos(3\omega_2 t)$	$\frac{A^3}{4}$	Potential Sub-Harmonic
11	$\cos\left[(2\omega_2+\omega_1)t\right]$	$\frac{3}{4}I\ A^2$	–
12	$\sin\left[(2\omega_2+\omega_1)t\right]$	$-\frac{3}{4}QA^2$	–
13	$\cos\left[(2\omega_1+\omega_2)t\right]$	$\frac{3}{4}A\left(I^2-Q^2\right)$	–
14	$\sin\left[(2\omega_1+\omega_2)t\right]$	$-\frac{3}{2}IQA$	–

In the context of receiver blocking, terms 1 and 2 in Table 1 are the most damaging because they are completely independent of the blocker's frequency. Since the blocker's impact is identical to another 3rd-order intermodulation term, receiver blocking will initially begin as a loss in signal-to-interference ratio rather than front-end gain-compression or impact to an individual stage's noise figure performance. Terms 3 – 6 can impact receiver performance if the blocking signal is at half or double that of the desired signal with a similar situation applying to term 10. The other terms in the table should be inconsequential to receiver performance.

The blocker's impact on the receiver's signal-to-interference ratio can be found by using the previous results in the context of (5). Only the third-order terms get involved for the general blocker-frequency case. The output power of the desired signal is given by

$$P_{desired}=k_1^2\left(\frac{I^2}{2R_o}+\frac{Q^2}{2R_o}\right) \tag{48}$$

The power associated with the blocking term (terms 1 and 2 in Table 1) is

$$P_{blocker}=k_3^2\left[\frac{9}{16}\frac{I^2A^4}{2R_o}+\frac{9}{4}\frac{Q^2A^4}{2R_o}\right]=k_3^2\frac{A^4}{2R_o}\left(\frac{9}{16}I^2+\frac{9}{4}Q^2\right) \tag{49}$$

In most digital communications, the signal power in the *I* and *Q* portions of the signal will be equal in which case from (43) the power in the desired signal is

$$P_{sig}=\frac{I^2}{2R_o}+\frac{Q^2}{2R_o}=P_{si}+P_{sq} \tag{50}$$

with $P_{si}=P_{sq}=P_{sig}/2$. Using this fact in (49) produces

$$P_{blocker}=k_3^2\frac{A^4}{2R_o}\left(\frac{9}{16}R_oP_{sig}+\frac{9}{4}R_oP_{sig}\right)=k_3^2\left(\frac{45}{32}\right)A^4P_{sig} \tag{51}$$

Combining this result with (50), the resultant signal-to-blocker power ratio is

$$\Lambda = \frac{P_{desired}}{P_{bloc\,\mathrm{ker}}} = \left(\frac{k_1}{k_3}\right)^2 \left(\frac{32}{45}\right)\left(\frac{1}{A^4}\right) \tag{52}$$

The blocker signal's amplitude can be expressed in terms of its power as $A = \sqrt{2R_o P_{bloc\,\mathrm{ker}}}$ which transforms (52) to

$$\Lambda = \left(\frac{32}{45}\right)\left(\frac{k_1}{k_3}\right)^2 \frac{1}{4R_o^2 P_{bloc\,\mathrm{ker}}^2} \tag{53}$$

This result is directly related to the input 3rd-order intercept point (27) thereby leading to

$$\Lambda_{dB} = 2\left(IIP3_{dBm} - P_{bloc\,\mathrm{ker}\_dBm}\right) - 3.98 \text{ dB} \tag{54}$$

Several numerical results are tabulated using (54) in Table 2.

Table 2 Maximum Blocker Level Relative to Input IP3 for Given S/IM Ratio

Target Λ_{dB}, dB	$IIP3_{dBm} - P_{bloc\,\mathrm{ker}\_dBm}$, dB
10	7
15	9.5
20	12
25	14.5
30	17
35	19.5

A large amount of potentially helpful nonlinear results can also be found in [9].

5 Cross-Modulation

Receiver blocking tests are performed with an unmodulated sinusoidal signal. If the blocking signal is modulated in amplitude and or phase, however, that modulation can manifest itself as an additional complication in the receiver's net signal to noise plus interference ratio (S/(N+I)).

Cross-modulation is usually characterized using the input signal [6]

$$e_i = A\left[1 + M\cos\left(\omega_m t\right)\right]\cos\left(\omega_1 t\right) + A\cos\left(\omega_2 t\right) \tag{55}$$

where *M* is the AM modulation index and ω_m is the radian frequency of the modulation. With AM modulation present through a nonlinear system, some of the amplitude modulation gets impressed on the unmodulated carrier at frequency ω_2 thereby resulting in an AM modulation index associated with that tone as

$$M' = \frac{3k_3 A^2 M}{k_1 + \frac{3}{4}k_3 A^2} \tag{56}$$

The cross-modulation factor *CM* is defined as

$$CM \equiv \frac{M'}{M} = \frac{3k_3A^2}{k_1 + \frac{3}{4}k_3A^2} \tag{57}$$

For very large signals, note that $CM \to 4$ which implies an increase in the modulation index! At much weaker signals, however,

$$CM \to 3\left|\frac{k_3}{k_1}\right|A^2 \tag{58}$$

In terms of decibel quantities, (58) can be expressed as

$$CM_{dB} = 20\log_{10}\left(CM\right) = 2\left(P_{carrier\_dBm} - IIP3_{dBm}\right) - 12 \text{ dB} \tag{59}$$

where

$$P_{carrier\_dBm} = 10\log_{10}\left(\frac{A^2}{2R_o}\right) + 30 \text{ dBm} \tag{60}$$

6 Noise Power Ratio (NPR)

The noise to power ratio (NPR) is normally associated with hard signal-limiting and is consequently often attributed to analog-to-digital converter (ADC) signal loading questions. Nyquist bandwidth Gaussian noise is assumed at the ADC input(s) and any clipping which occurs is assumed to create a white noise spectrum which is spread equally across the Nyquist bandwidth.

A complete discussion and derivation of NPR is given in [8]. The NPR is given by[2]

$$NPR_{dB} = 10\log_{10}\left(\frac{\sigma^2}{N_T}\right) \text{ dB} \tag{61}$$

where σ^2 is the input variance of the noise and

$$N_T = \frac{\left(k\sigma\right)^2}{3\,2^{2n}} + 2\sigma^2\left(k^2+1\right)\left[1 - N\left(k\right)\right] - k\sigma^2\sqrt{\frac{2}{\pi}}\exp\left(-\frac{k^2}{2}\right) \tag{62}$$

Note also that

$$k = \frac{ADC\ Peak\ to\ Peak\ Maximum\ Input, V}{2\sigma} \tag{63}$$

$$N\left(k\right) = \int_{-\infty}^{k} \frac{\exp\left(-\frac{t^2}{2}\right)}{\sqrt{2\pi}} dt \tag{64}$$

Graphical results using (61) are provided in Figure 6.

[2] Brute-force time domain simulation of NPR done in u21625_exciter_npr.m. Time domain NPR-related simulation done using tanh() nonlinearity in u22005_exciter_npr.m also. RF devices exhibit a soft nonlinearity as compared to the abrupt-limiting associated with ADCs as discussed here.

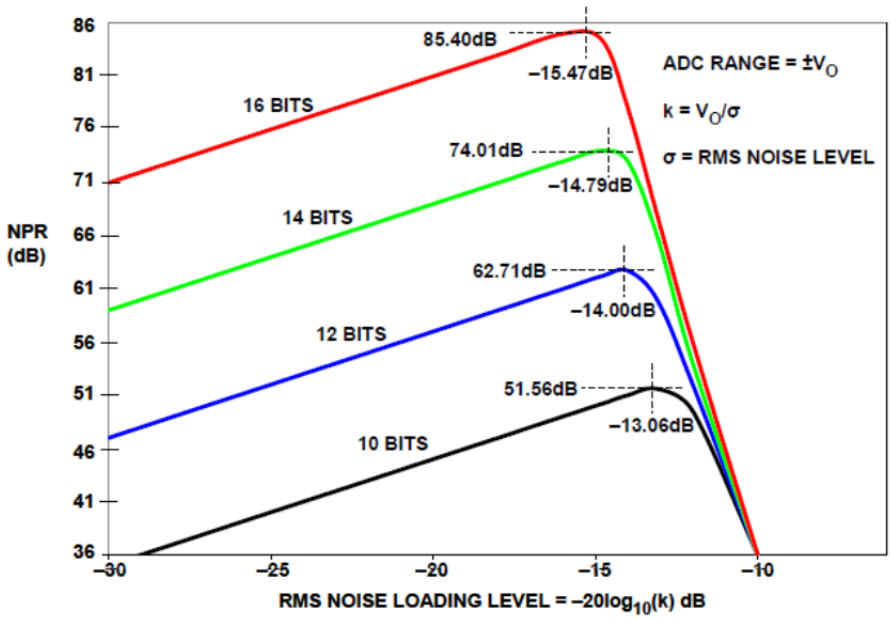

Figure 6 Theoretical NPR for 10, 12, 14, and 16-bit ADCs [8]

Table 3 Theoretical Maximum NPR [8]

ADC Bits	Optimum *k*	Optimum *k*, dB	Max NPR, dB
8	3.92	11.87	40.60
9	4.22	12.50	46.05
10	4.50	13.06	51.56
11	4.76	13.55	57.12
12	5.01	14.00	62.71
13	5.26	14.41	68.35
14	5.49	14.79	74.01

6.1 NPR for RF Block Exhibiting tanh() Nonlinearity

A detailed discussion of NPR in this present context was done elsewhere [9]. Pertinent results are copied below.

Under the NPR testing conditions, it was mathematically determined:

- Single-Tone 1 dB Compression Point = P_{1dB}
- Power Level at which Output Waveform Achieves 37 dB NPR = P_{1dB} – 8.76 dB
- Output Peak Envelope Power under NPR Conditions = P_{1dB} – 3 dB

Different nonlinear characteristics will result in different results of course, but based upon these results, the modulated signal power must be kept a minimum of about 10 dB below the sinusoidal output 1 dB compression point in order to achieve a NPR of 37 dB. The back-off amount may be even larger if soft-limiting stages are cascaded. An example one-sided computed power spectral density spectrum which is NPR = 37 dB compliant is shown in Figure 7.

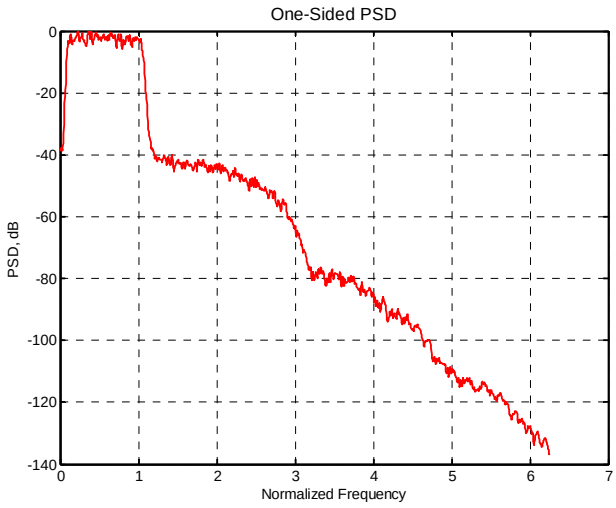

Figure 7 Example NPR-compliant one-sided power spectral density[3]

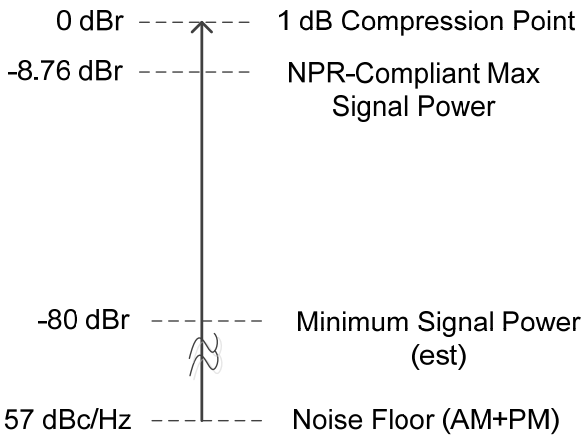

Figure 8 Relative signal levels involved for WCEX[4]

A number of results based upon the material in [9] are collected in Table 4 and partially plotted in Figure 9. As shown there, only about 0.12 dB of gain compression can be tolerated with a hyperbolic tangent nonlinearity if an *NPR* of 40 dB is desired. These results illustrate how difficult achieving an *NPR* > 30 dB really is.

These results apply for a single hyperbolic tangent nonlinearity characteristic and therefore do not include any benefit from digital signal processing. Reference is made to parameter γ in Table 4 which plays a role in the assumed hyperbolic tangent function nonlinearity between input and output voltages as

$$v_{out}(t) = \tanh\left[\gamma v_{\text{in}}(t)\right] \tag{65}$$

Table 4 Hyperbolic Tangent and NPR[5]

γ	$P_{1dB} - P_{in}$, dB	P_{in}, dBm	P_{out}, dBm	Gain, dB	*PEP*, dBm	*PAR, dB*	*NPR*, dB
0.1	18.06	–13.46	–13.48	–0.02	–7.18	6.30	57
0.2	12.04	–7.44	–7.51	–0.07	–1.31	6.20	45
0.25	10.10	–5.50	–5.62	–0.12	0.47	6.09	41.4
0.3	8.51	–3.91	–4.09	–0.18	1.59	5.68	38
0.36	6.93	–2.33	–2.57	–0.24	3.57	6.14	35.4
0.4	6.02	–1.42	–1.71	–0.29	3.70	5.41	33
0.5	4.08	0.52	0.072	–0.45	5.56	5.49	30
0.60	2.50	2.10	1.48	–0.62	6.57	5.09	27.5
0.70	1.16	3.44	2.63	–0.81	7.40	4.77	25.4
0.7126	1.00	3.60	2.76	–0.84	7.70	4.94	25.1
0.80	**0.00**	4.60	3.58	–1.02	8.26	4.68	23.7
0.85	–0.53	5.13	4.00	–1.13	8.51	4.51	22.9
1.00	–1.94	6.54	5.08	–1.46	9.74	4.66	21.0
1.25	–3.88	8.48	6.43	–2.05	10.33	3.90	18.3

[3] From u21625_exciter_npr.m.
[4] From U21661 Figures for U21660.vsd.
[5] Using u22005_exciter_npr.m. Note that the 1 dB compression point corresponds to $\gamma = 0.7126$ from [9]. Calculations performed using u22005_exciter_npr.m. Modulated signal assumed to be filtered Gaussian noise having a baseband bandwidth of 480 kHz. PEP measured by applying a square-law detector followed by a stiff post-detection lowpass filter having a bandwidth of 192 kHz. Wider post-detection filter needed to more accurately capture the peaks.

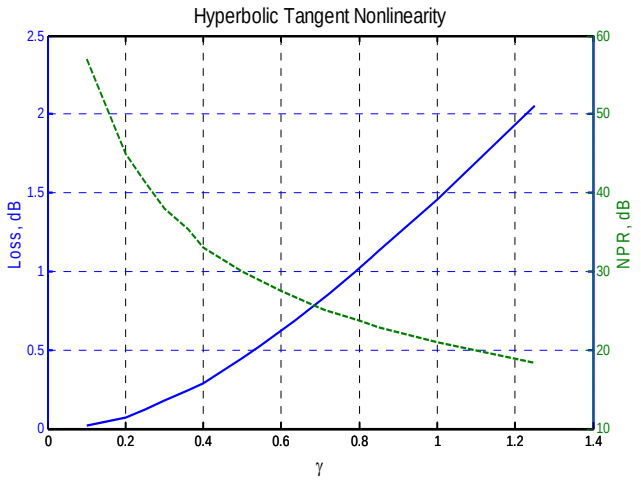

Figure 9 Stage loss (dB) and NPR (dB) versus γ from[6] Table 4

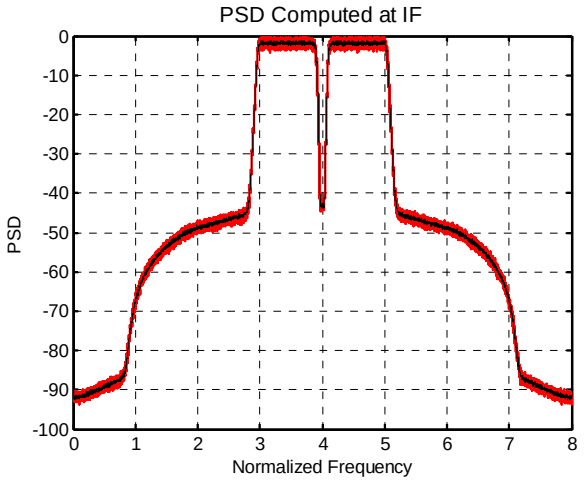

Figure 10 Full power spectral density with carrier centered at x = 4 for γ = 0.25. NPR is about 40 dB as shown.

These results can be used in the receiver design by keeping track of the 1 dB compression point for the entire receive chain (which is directly related to the input 3rd-order intercept point) in allocating a necessary AGC profile. Once a profile has been determined, the receiver's nonlinear performance versus desired and undesired signal levels and offset frequency can be ascertained.

7 Error Vector Magnitude

Error vector magnitude (EVM) was originally addressed in [1] and those results reflected forward to [9]. This information is repeated here once more.

IQ modulation accuracy (i.e., gain and phase) is intimately tied to EVM performance and to a lesser degree to NPR performance. Modulation accuracy and EVM are most critical for single-carrier systems as compared to say OFDM systems. EVM and I,Q errors are mathematically related as[7]

$$EVM_{\%rms} = \sqrt{\frac{\overline{I_{errors}^2 + Q_{errors}^2}}{\overline{I^2 + Q^2}}} \times 100\% \tag{66}$$

In the context of IQ phase imbalance θ and gain imbalance ΔG_{dB} where[8]

$$g = 10^{0.05\Delta G_{dB}} \tag{67}$$

$$\rho = g^2 = \left(\frac{1+\frac{\delta}{2}}{1-\frac{\delta}{2}} \right)^2 \tag{68}$$

[6] u22005_exciter_npr.m.
[7] [1], equation (5A.8).
[8] [1], equations (5A.2) and (5A.5).

$$\delta = \frac{4\sqrt{\rho} - 2 - 2\rho}{1 - \rho} \tag{69}$$

EVM and gain/phase imbalance are related as[9]

$$EVM_{\%rms} = \sqrt{2 - 2\cos\left(\frac{\theta}{2}\right) + \left(\frac{\delta}{2}\right)^2} \times 100\% \tag{70}$$

At first glance, it may appear redundant to specify EVM, gain-phase imbalance, and modulation bandwidth flatness, but EVM is primarily intended to address digital modulation cases whereas the others are most helpful with analog waveforms.

Gain and phase mismatch play an integral part in contributing to EVM as shown in Figure 11, and the EVM sets the limit on the achievable bit error rate floor (with no FEC present). Based upon the definition given in (66), the EVM is directly related to the achievable symbol-to-noise ratio ceiling as

$$\frac{E_s}{N} \le \frac{1}{\left(0.01 EVM_{\%rms}\right)^2} \tag{71}$$

The symbol error rate for 16-QAM and 64-QAM assuming local oscillator related phase noise is present is shown in Figure 12 and Figure 13 respectively. Equation (70) can be used to relate the RMS phase noise quantities shown in the figures back to an equivalent EVM as tabulated in Table 5. Performance loss at an ideal symbol error rate of 10^{-5} is also tabulated in the table for the 16-QAM and 64-QAM.

The performance loss values given in Table 5 need to be viewed in a whole-system context. In the single carrier case, the carrier recovery portion of a coherent receiver will track out much of the close-in phase noise if the E_s / N is primarily being limited by phase noise. The same can be said of multi-carrier OFDM systems so long as the symbol rate is adequately high. No such forgiveness is present for nonlinearities present in the system unless specific algorithms are used to compensate for would-be offending nonlinearities.

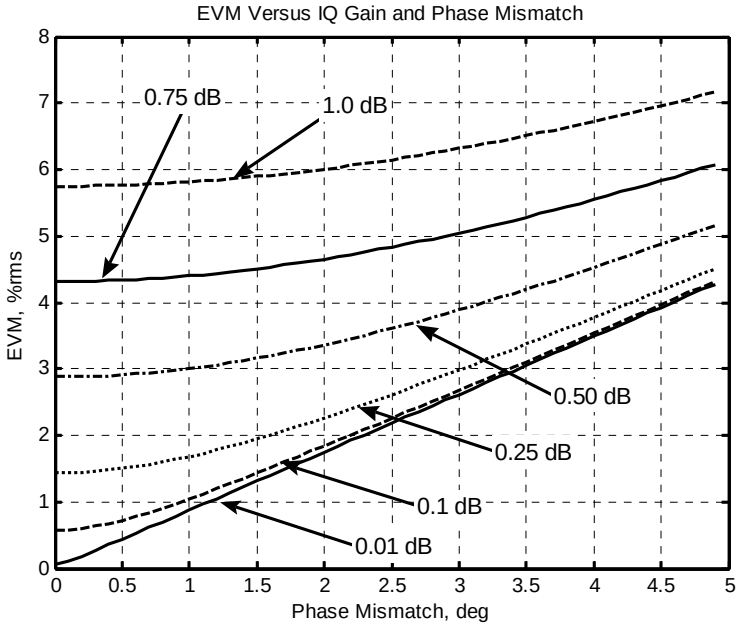

Figure 11 IQ gain and phase mismatch contribution to EVM[10]

[9] [1], equation (5A.10).

Table 5 Equivalent EVM Versus Phase Noise[11]

Phase Noise, ° RMS	Equivalent EVM, % RMS from (70)	E_s / N, dB from (71)	*16-QAM Perform Loss, dB*	*64-QAM Perform Loss, dB*
0.5	0.436	47.2	≈ 0	0.2
1.0	0.873	41.2	0.1	1.0
1.5	1.31	37.7		3.5
2	1.75	35.1	0.8	>> 6
3	2.62	31.6	2.4	
4	3.49	29.1	7.0	
5	4.36	27.2		

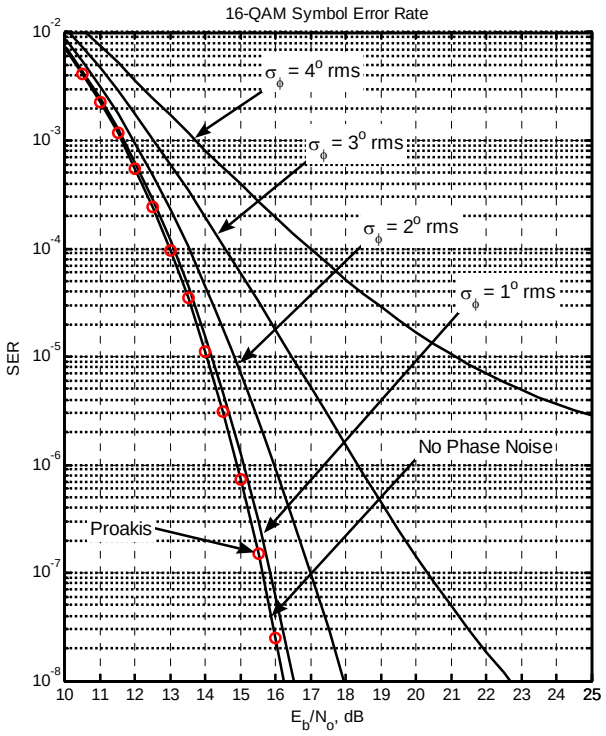

Figure 12 16-QAM symbol error rate with phase noise present[12]

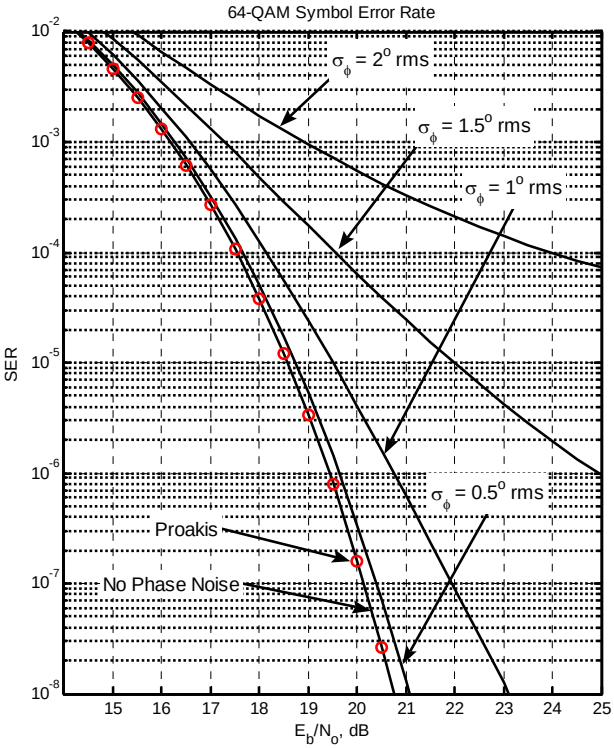

Figure 13 64-QAM symbol error rate with phase noise present[13]

8 AM Demodulation

Amplitude modulation is still used in some systems for analog communication. Although multiple demodulation methods are possible, only the square-law and envelope detection methods are considered here.

In the case of a single-tone modulation, the output signal-to-noise ratio for the tone is given by[14]

[10] From [1], computed using Book CD:\Ch5\u13149_iq_imbal_evm.m.
[11] Performance loss is estimated from Figure 12 and Figure 13 at an ideal SER of 10^{-5}.
[12] Figure 2-36 from [1].
[13] Figure 2-37 from [1].
[14] Notes in U22794 AM Square-Law Detector.pdf.

$$\gamma_{out} = \frac{1}{2} \frac{m_0^2 \, \gamma_{carr}}{\frac{3}{16} \frac{1}{\gamma_{carr}} + \frac{m_0^2}{4} + \frac{1}{2}} \tag{72}$$

where

$$\gamma_{carr} = \gamma_{in} \frac{2}{2 + m_0^2} \tag{73}$$

γ_{in}	Input signal to noise ratio
γ_{carr}	Carrier-only input signal to noise ratio
m_0	Modulation index

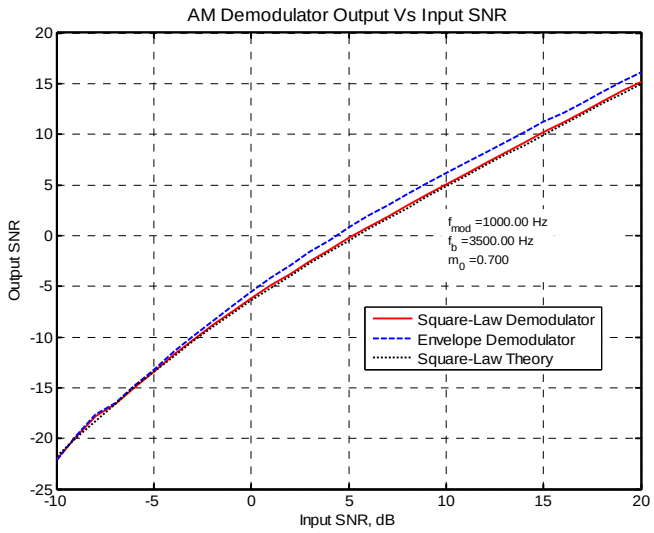

Figure 14 Example input versus output SNR for AM demodulation[15] with 0.70 modulation index

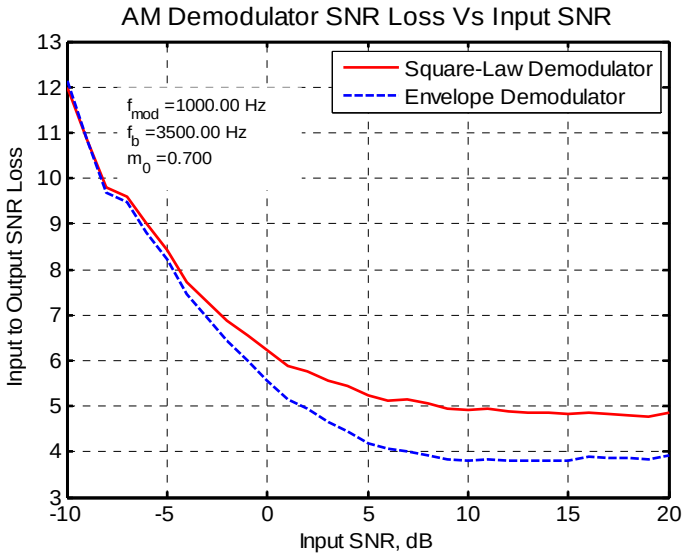

Figure 15 Output SNR loss versus input SNR for 0.70 modulation index, corresponding to Figure 14

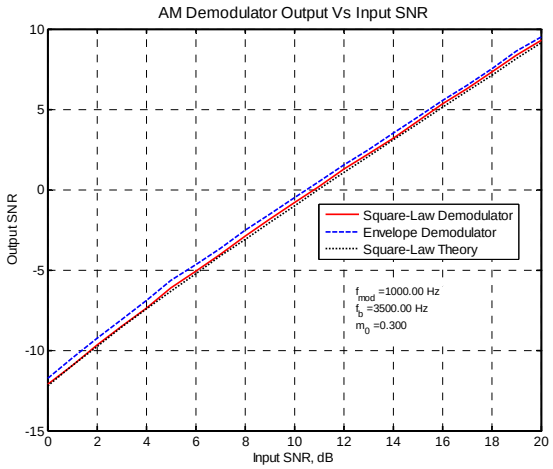

Figure 16 AM detector output SNR versus input SNR for a 0.30 modulation index

[15] From u22793_am_sensitivity.m.

9 FM Demodulation

FM demodulation has been studied and analyzed extensively over the years. The standard definition for *FM threshold* is difficult, however, because this is defined differently by different researchers.

The FM demodulation subject is addressed here by considering the performance of several specific mathematical implementations for the demodulator and the single-tone case alone is considered. Several parameter definitions are needed:

Δf	Peak frequency deviation, Hz
f_m	Frequency modulation rate, Hz. ω_m is the radian frequency equivalent
f_B	Pre-detection IF bandwidth = 2 f_B
f_L	Post-demodulator highpass corner frequency, Hz
f_H	Post-demodulator lowpass corner frequency, Hz
A_o	Signal voltage amplitude, V
β	Modulation index given by $\Delta f \ / \ f_m$
ω_o	Radian carrier frequency, rad/sec
η_o	One-sided noise spectral density, dBm/Hz
R_o	Standard impedance level, 50Ω
T_s	Time increment between signal samples, sec
k	Digital sample index, an integer

The instantaneous frequency for the single-tone case is subsequently given by

$$f_{inst}(t) = \Delta f \cos(\omega_m t) \tag{74}$$

from which the instantaneous phase is given by

$$\theta(t) = \beta \sin(\omega_m t) \tag{75}$$

The ideal signal is consequently given by

$$\begin{aligned} s(t) &= A_o \cos\left[\omega_o t + \beta \sin(\omega_m t)\right] \\ &= A_o \cos\left[\beta \sin(\omega_m t)\right] \cos(\omega_o t) - A_o \sin\left[\beta \sin(\omega_m t)\right] \sin(\omega_o t) \\ &= I(t) \cos(\omega_o t) - Q(t) \sin(\omega_o t) \end{aligned} \tag{76}$$

where

$$\begin{aligned} I(t) &= A_o \cos\left[\beta \sin(\omega_m t)\right] \\ Q(t) &= A_o \sin\left[\beta \sin(\omega_m t)\right] \end{aligned} \tag{77}$$

From (76), the power of the desired signal is $P_{sig} = A_o^2 / 2$ whereas the total noise power falling through the pre-detection IF filter is given by $P_{noise} = 2\eta_o f_B$.

It is convenient to express the noise falling through the IF filter in a similar fashion as

$$n(t) = n_i(t) \cos(\omega_o t) - n_q(t) \sin(\omega_o t) \tag{78}$$

where the total noise power is given by

$$P_{noise} = \frac{\widetilde{n_i^2}}{2} + \frac{\widetilde{n_q^2}}{2} = 2\eta_o f_B R_o \tag{79}$$

and the n_i and n_q functions are appropriately band-limited Gaussian noise processes.

9.1 FM Demodulator Derivation

In terms of in-phase (I) and quadrature-phase (Q) signals, the instantaneous phase is given by

$$\phi(t) = \tan^{-1}\left(\frac{Q}{I}\right) \tag{80}$$

and the associated instantaneous frequency is given by

$$\omega(t) = \frac{d\phi}{dt} = \frac{IQ' - QI'}{I^2 + Q^2} \tag{81}$$

where the apostrophes denote time-differentiation. Several options are possible in taking the next computational step.

The first option is to simply approximate the time-derivatives as

$$\begin{aligned} I' &\approx \frac{I_k - I_{k-1}}{T_s} \\ Q' &\approx \frac{Q_k - Q_{k-1}}{T_s} \end{aligned} \tag{82}$$

Substituting (82) into (81) produces the first FM demodulator approximation

$$f_k = \frac{1}{2\pi T_s}\frac{Q_k I_{k-1} - I_k Q_{k-1}}{I_k^2 + Q_k^2} \tag{83}$$

Of course high-order approximation can be used for the approximate time-derivatives in (82), but (83) is a frequent approximation that is seen in the literature.

The second FM demodulator approximation considers the precise phase difference between two complex sample pairs denoted here by (I_k, Q_k) and (I_{k-1}, Q_{k-1}). The product between these two samples (conjugating the second sample) is precisely given by

$$\begin{aligned} \left(I_k + jQ_k\right)\left(I_{k-1} - jQ_{k-1}\right) &= A_k e^{j\phi_k} A_{k-1} e^{-j\phi_k} \\ &= A_k A_{k-1} \exp\left[\, j\left(\phi_k - \phi_{k-1}\right)\right] \end{aligned} \tag{84}$$

Taking the phase argument on each side of (84) produces

$$\Delta\phi = \tan^{-1}\left(\frac{Q_k I_{k-1} - I_k Q_{k-1}}{I_k I_{k-1} + Q_k Q_{k-1}}\right) \tag{85}$$

and the associated instantaneous frequency given by

$$f_k = \frac{\Delta\phi}{2\pi T_s} \tag{86}$$

For the third and final approximate FM demodulator, it is assumed that a slow-AGC is present which keeps the average input power level to the FM demodulator constant. This is equivalent to roughly assuming that the denominator portion of (83) is constant, leading to the approximate FM demodulator formula given by

$$f_k = \frac{1}{2\pi T_s \sigma_{sig}^2}\left(Q_k I_{k-1} - I_k Q_{k-1}\right) \tag{87}$$

where

$$\sigma_{sig}^2 = \widetilde{\left(I^2 + Q^2\right)} \tag{88}$$

The onset of FM threshold (regardless of the precise definition) is always associated with *FM clicks* which correspond to signal trajectories which pass through or extremely close to the origin of the (*I*, *Q*) plane. Such trajectories correspond to the denominator portion of (83) being zero or extremely small.

In the results that follow, 7th-order Chebyshev lowpass filters with a ripple of 0.01 dB were used to create the bandlimited noise (applied to n_i and n_q in (78)). A cascade of a 5th-order highpass and lowpass Chebyshev filter (ripple 0.01 dB) were used to post-filter the demodulator's output.

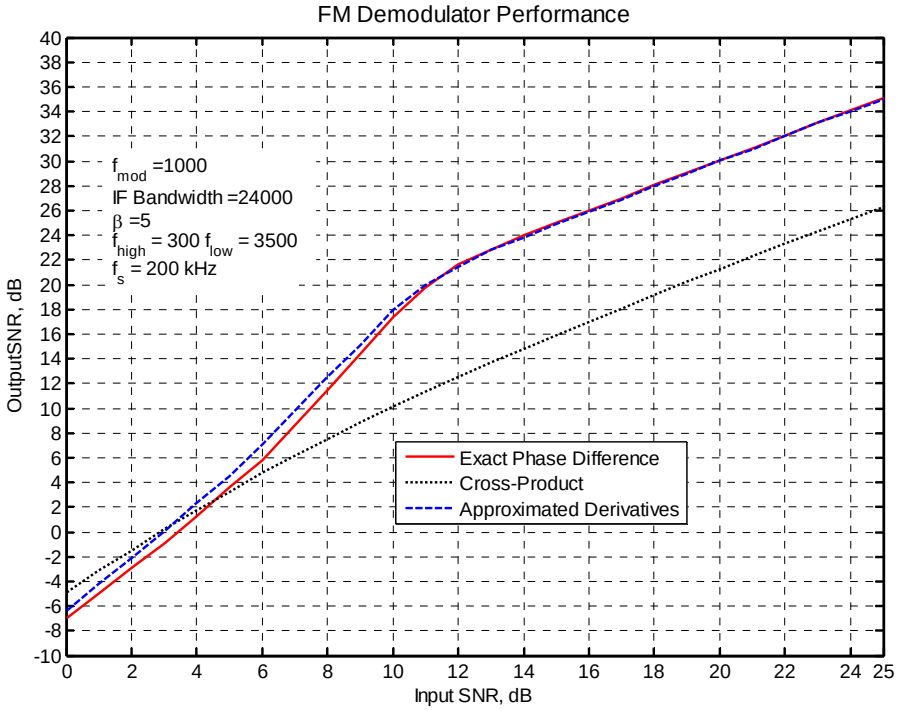

Figure 17 FM demodulator performance using a wide IF bandwidth of 24 kHz. Output SNR is about 24 dB for an input SNR[16] of 14.

[16] Noise measured within the IF bandwidth. Using u22800_fm_sensitivity.m.

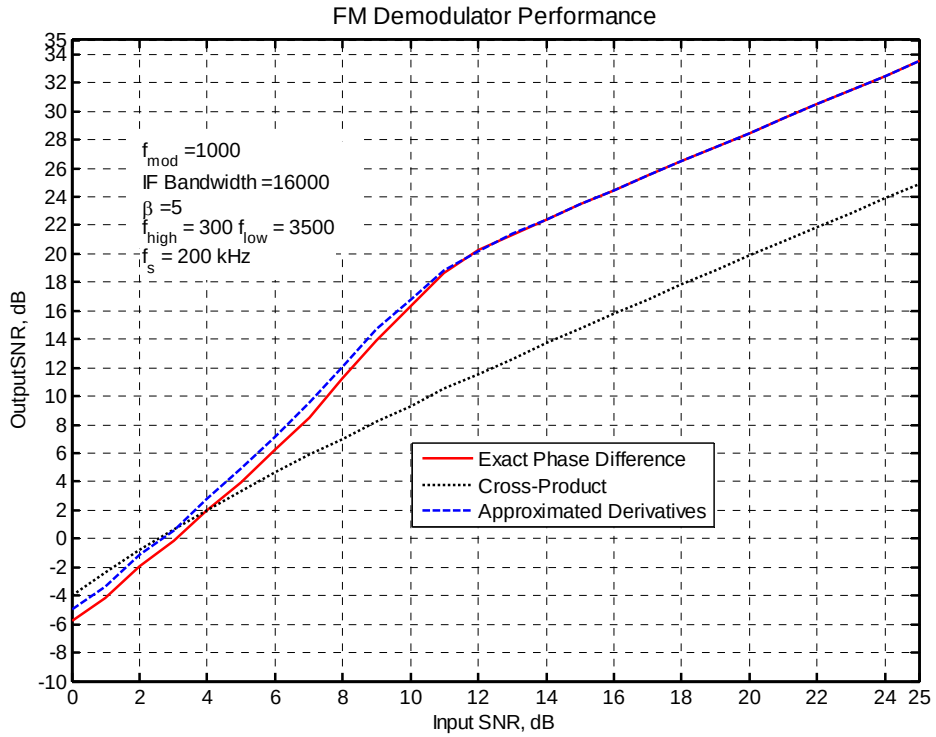

Figure 18 FM demodulator performance using an IF bandwidth of 16 kHz

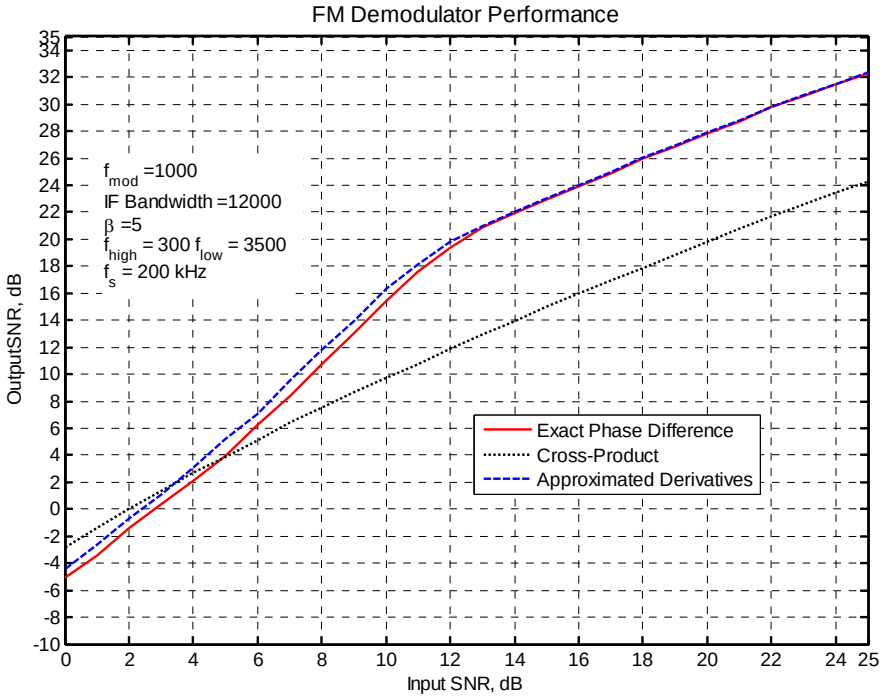

Figure 19 FM demodulator performance using an IF bandwidth of 12 kHz

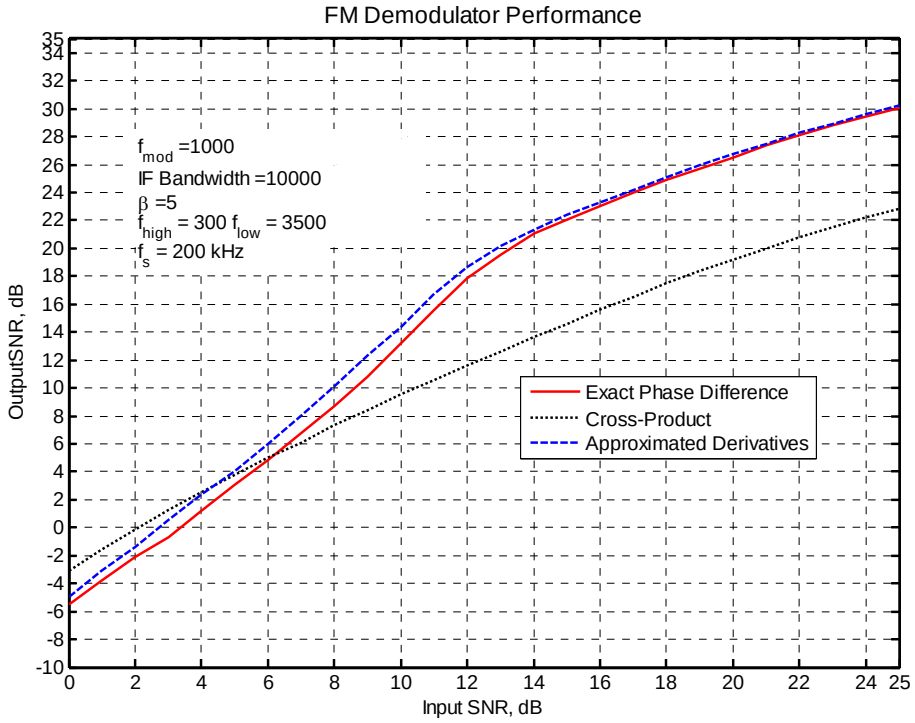

Figure 20 FM demodulator performance using an IF bandwidth of 10 kHz

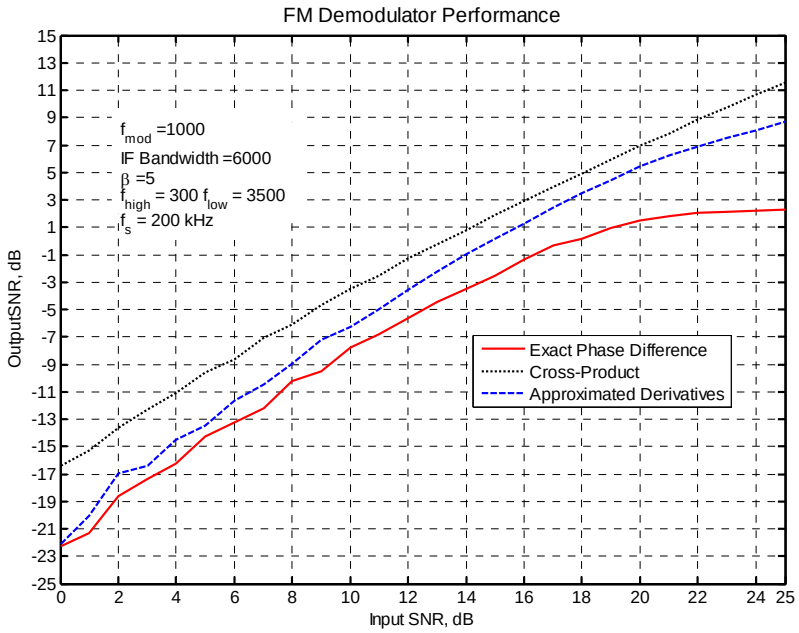

Figure 21 Insufficient IF bandwidth crushes FM demodulator performance

10 Reciprocal Mixing

Reciprocal mixing as it applies to the main local oscillator's phase noise performance is addressed in detail in §5.3 of [1]. The situation is shown in Figure 22 where a strong interfering signal is heterodyned in frequency by the local oscillator's phase noise sidebands. The effect of phase noise upon the desired signal is to create a cross-channel noise term in the resultant baseband *I* and *Q* channels thereby resulting in baseband power spectral densities of

$$\begin{aligned} S_{I\_tot}(f) &= S_I(f) + S_Q(f) \otimes S_\theta(f) \\ S_{Q\_tot}(f) &= S_Q(f) + S_I(f) \otimes S_\theta(f) \end{aligned} \tag{89}$$

where $S_I(f)$ and $S_Q(f)$ are the ideal baseband power spectral densities in the absence of any phase noise impairments and $\otimes$ represents frequency-domain convolution.

At larger offset frequencies from the desired signal, the phase noise sidebands can cause strong off-channel signal energy to be heterodyned directly upon the desired channel. A rectangular out-of-band signal spectrum and Lorentzian LO phase noise spectrum are assumed in §5.3 of [1] to consider this situation further. More specifically, the power spectral density of the LO phase noise is assumed to be

$$S_\theta(f) = L_{floor} + \frac{L_o}{1 + \left(\frac{f}{f_c}\right)^2} + \delta(f) \tag{90}$$

where L_{floor} and L_o have units of rad^2/Hz since the ideal carrier term has unity-power. Assuming that the RF interfering signal has a rectangular spectrum with an RF bandwidth of *2B* Hz, frequency offset of Δf_{sep}, and a main-lobe power spectral density of L_x W/Hz, the resultant spectrum which is ultimately translated to baseband has a power spectral density of

$$S_{bb}(f) = 2BL_xL_{floor}\delta(f) + f_cL_oL_x\left[\tan^{-1}\left(\frac{f + B - \Delta f_{sep}}{f_c}\right) - \tan^{-1}\left(\frac{f - B - \Delta f_{sep}}{f_c}\right)\right] \tag{91}$$

An illustrative example of (91) is shown in Figure 23. As the interfering signal's frequency offset Δf_{sep} becomes larger compared to the Lorentzian bandwidth parameter f_c and signal bandwidth parameter *B*, the spectrum reflected to baseband becomes increasingly flat.

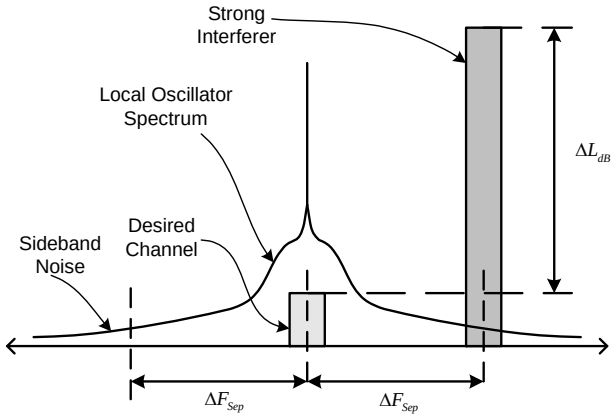

Figure 22 Strong interfering channels are heterodyned on top of the desired receive channel by local oscillator sideband noise

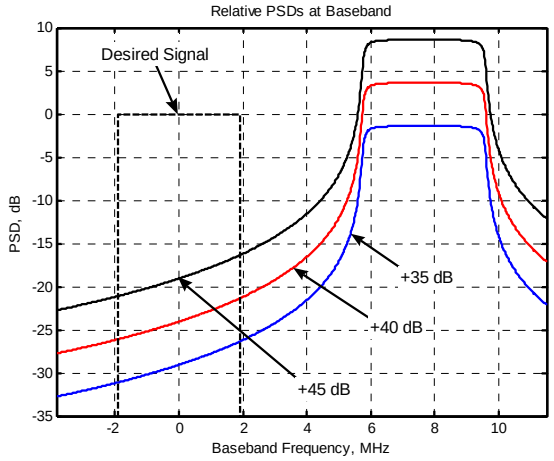

Figure 23 Example baseband spectra[17] caused by reciprocal mixing between a strong interferer that is offset 4*B* Hz higher in frequency than the desired signal and stronger than the desired signal by the dB amounts shown.

If (91) is integrated across the entire baseband matched-filter bandwidth (–*B*, *B*), the resultant interference power competing with the desired signal is given by

$$\sigma_{MFX}^2 = 4B^2 L_x L_{floor} + L_x L_o f_c \left[g\left(\frac{a_1+B}{f_c}\right) - g\left(\frac{a_1-B}{f_c}\right) - g\left(\frac{a_2+B}{f_c}\right) + g\left(\frac{a_2-B}{f_c}\right) \right] \tag{92}$$

where

$$\begin{aligned} a_1 &= B - \Delta f_{sep} \\ a_2 &= -B - \Delta f_{sep} \end{aligned} \tag{93}$$

$$g(u) = f_c \left[u \tan^{-1}(u) - \frac{1}{2}\log_e\left(1+u^2\right) \right] \tag{94}$$

It is convenient to think of the interfering signal being $\Delta L_{dB} = 10\log_{10}(\chi)$ stronger than the desired signal as shown in Figure 22. As shown in §5.3 of [1], the resultant receiver SNR is finally given by

$$SNR_{out} = \left[\frac{1}{SNR_{in}} + \frac{\sigma_{MFX}^2}{2BL_{IQ}} \right]^{-1} \tag{95}$$

where

$$\frac{\sigma_{MFX}^2}{2BL_{IQ}} = \chi \left\{ 2BL_{floor} + \frac{L_o f_c}{2B} \left[g\left(\frac{a_1+B}{f_c}\right) - g\left(\frac{a_1-B}{f_c}\right) - g\left(\frac{a_2+B}{f_c}\right) + g\left(\frac{a_2-B}{f_c}\right) \right] \right\} \tag{96}$$

[17] Book [1] CD:\Ch5\u13157_rx_desense.m. Lorentzian spectrum parameters: L_o = –90 dBc/Hz, f_c = 75 kHz, L_{Floor} = –160 dBc/Hz, B = 3.84/2 MHz.

There are a number of parameters involved with using this final result (95) and some assumptions must be made in order to gain any further insight. Local oscillator phase noise parameters $f_c, L_o,$ and L_{floor} can be related back directly to the performance of the associated frequency synthesizer. This leaves only $B,\ \Delta f_{sep},$ and ΔL_{dB} remaining to be identified which is relatively straight forward based upon desired receiver envisioned scenarios.

Approximate expectations for representative phase noise performance are summarized in Table 6. Several (RF) modulation bandwidths have been set up in the interim as given in Table 7. Several example results are shown in Table 8 and Table 9 where the independent variable is frequency separation of the interferer with respect to the desired signal. Additional results are shown in Table 10 where $\Delta f_{sep} = 4B$ is held constant but ΔL_{dB} is swept.

Table 6 Synthesizer Approximated Phase Noise Expectations

LO Case	*Synthesizer Output Frequency, GHz*	*L_o, dBc/Hz*	*L_{floor}, dBc/Hz*	*f_c, kHz*
1	4 – 8	–115	–160	750
2	2 – 4	–120	–160	200
3	2 – 4	–110	–155	750
4	1 – 2	–125	–165	200
5	1 – 2	–115	–160	750
6	0.50 – 1.0	–130	–165	200
7	0.50 – 1.0	–120	–165	750

Table 7 Interim Modulation Bandwidth Cases

Modulation Bandwidth Case	*RF Bandwidth, MHz*
1	0.2
2	1.0
3	5.0
4	20.0

Table 8 Reciprocal Mixing for Input SNR = 12 dB, LO Case = 4, and Interferer 70 dB Above Desired. (RF modulation bandwidth for desired signal and interferer both equal to *2B*.)

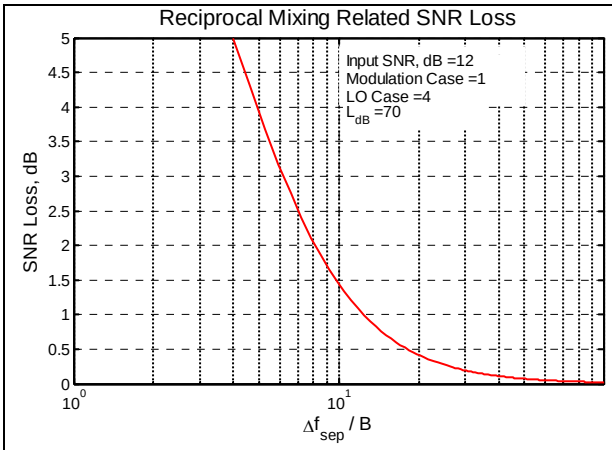

Figure 24 RF modulation bandwidth = 200 kHz

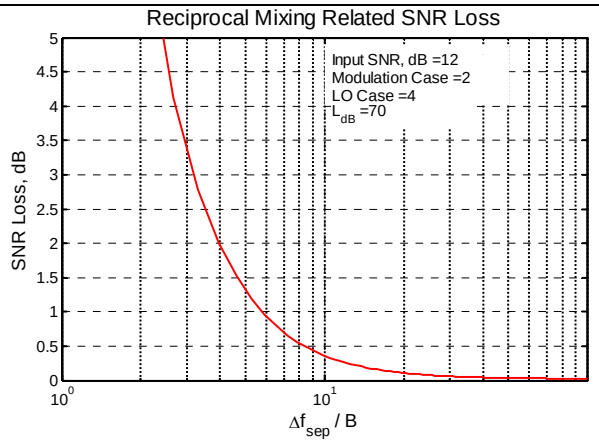

Figure 25 RF modulation bandwidth = 1 MHz

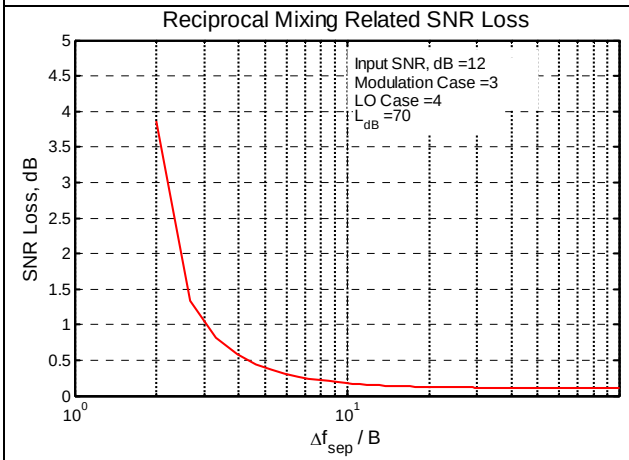

Figure 26 RF modulation bandwidth = 5 MHz

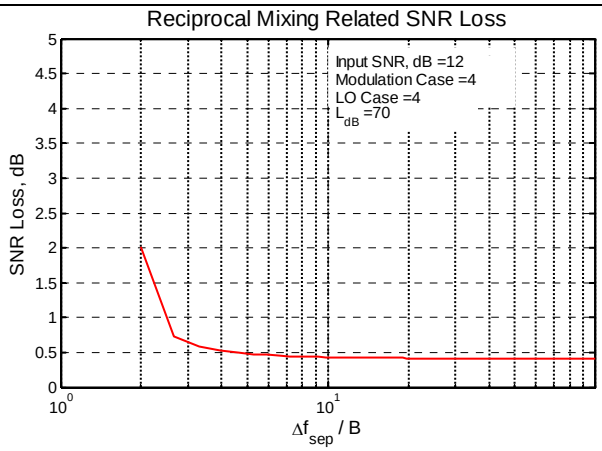

Figure 27 RF modulation bandwidth = 20 MHz

Table 9 Same as Table 8 Except LO Case = 6. (RF modulation bandwidth for desired signal and interferer both equal to *2B*.)

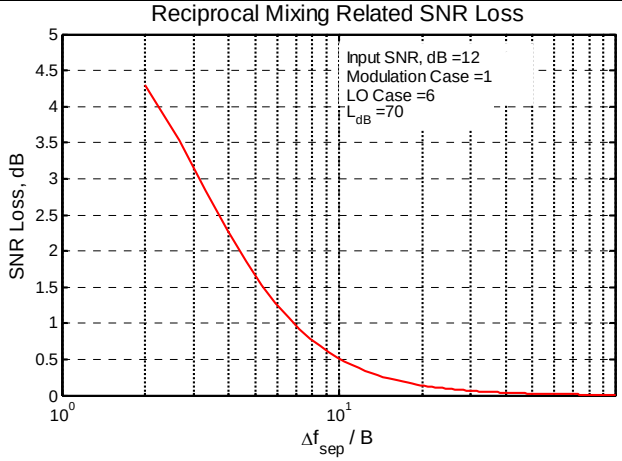

Figure 28 RF modulation bandwidth = 200 kHz

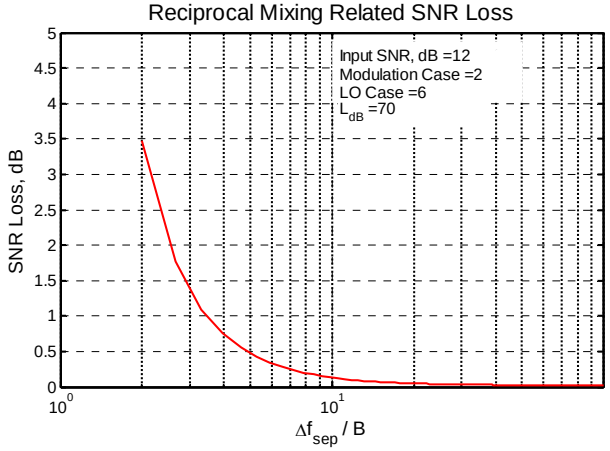

Figure 29 RF modulation bandwidth = 1 MHz

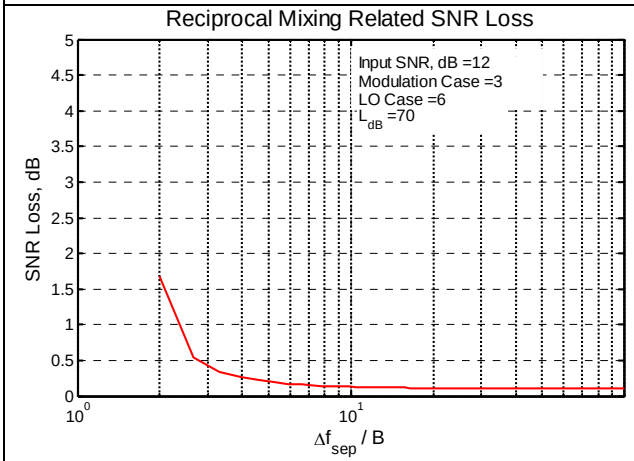

Figure 30 RF modulation bandwidth = 5 MHz

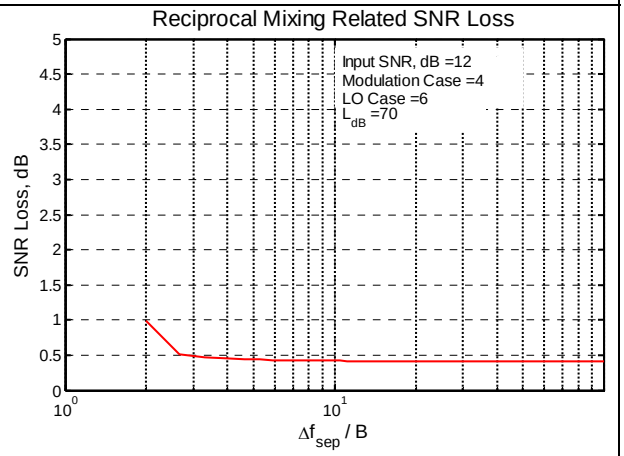

Figure 31 RF modulation bandwidth = 20 MHz

Table 10 Reciprocal Mixing for LO Case = 4, and frequency separation $\Delta f_{sep} = 4B$. (RF modulation bandwidth for desired signal and interferer both equal to *2B*.)

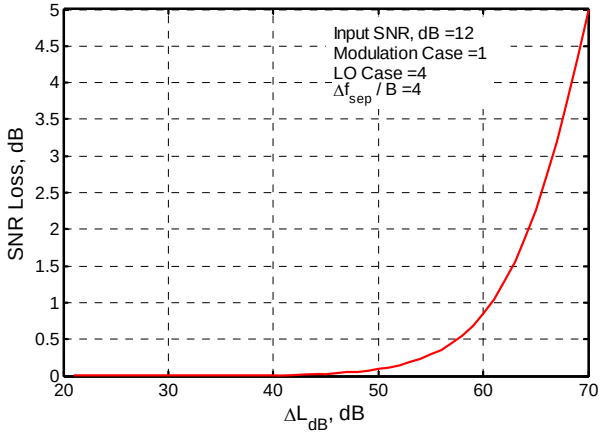

Figure 32 RF modulation bandwidth = 200 kHz. Input SNR = 12 dB.

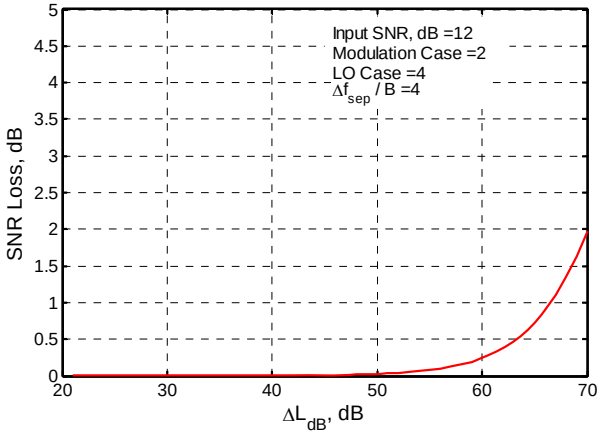

Figure 33 RF modulation bandwidth = 1 MHz. Input SNR = 12 dB.

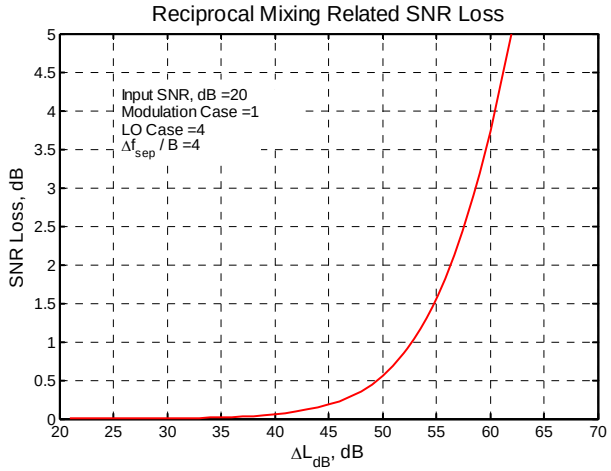

Figure 34 RF modulation bandwidth = 200 kHz, input SNR = 20 dB

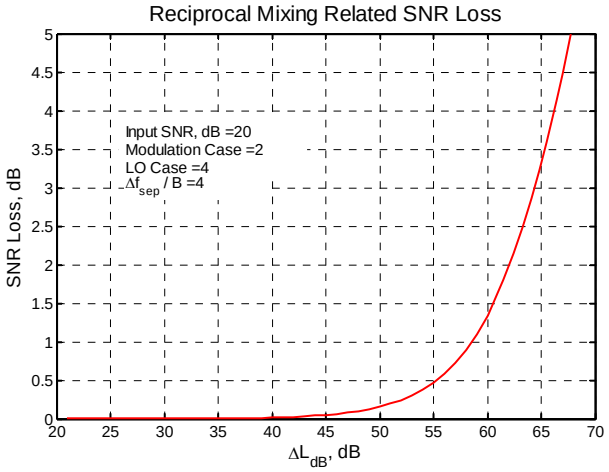

Figure 35 RF modulation bandwidth = 1 MHz, input SNR = 20 dB

11 Clock Phase Noise Impact on ADC Performance

This topic is covered in §5.10 of [1] and only some final results are provided here. ADC clock noise can pose serious issues in high dynamic range systems, particularly for higher bandwidth systems. Assuming that the power spectral density of the input signal to the ADC is given by $S_V(f)$ and the phase noise power spectral density of the clock's phase noise is given by $S_{\delta\theta}(f)$, the resultant signal power spectral density seen after the ADC conversion (infinitely fine quantization assumed along with no Nyquist-related folding) is

$$S_{Vn}(f) = \left(\frac{1}{2\pi f_s}\right)^2 \left[(2\pi f)^2 S_V(f)\right] \otimes S_{\delta\theta}(f) \text{ with } |f\ T_s| < \frac{1}{2} \tag{97}$$

Assume now that a strong interfering signal spectrum at the ADC input is rectangular in frequency and given by

$$S_V(f) = \begin{cases} \frac{L_x}{2B} & |f - f_o| \le B \\ 0 & otherwise \end{cases} \tag{98}$$

Further assume that the nominal clock frequency is f_s and that the phase noise spectrum of the clock-jitter is Lorentzian in nature. The corresponding power spectral density for the time-jitter is then

$$S_{\delta t}(f) = \frac{L_o}{(2\pi f_s)^2 \left[1 + \left(\frac{f}{f_c}\right)^2\right]} \tag{99}$$

Performing the frequency-domain convolution as given in (97) creates the resultant noise spectrum seen at the ADC's output given by

$$P_n(f) = \frac{f_c L_o}{2B f_s^2}\left[F\left(\frac{f_o + B - f}{f_c}, f_c, f\right) - F\left(\frac{f_o - B - f}{f_c}, f_c, f\right)\right] \tag{100}$$

in which

$$F(x,a,b) = a^2 x + \left(b^2 - a^2\right)\tan^{-1}(x) + ab\log_e\left(1 + x^2\right) \tag{101}$$

The clock's phase noise creates an increasing noise floor spectrum beneath the strong interfering signal which extends down to low frequencies as well as shown in the example of Figure 36. Consequently, this interferer-broadening can degrade the performance of IQ baseband ADCs as well.

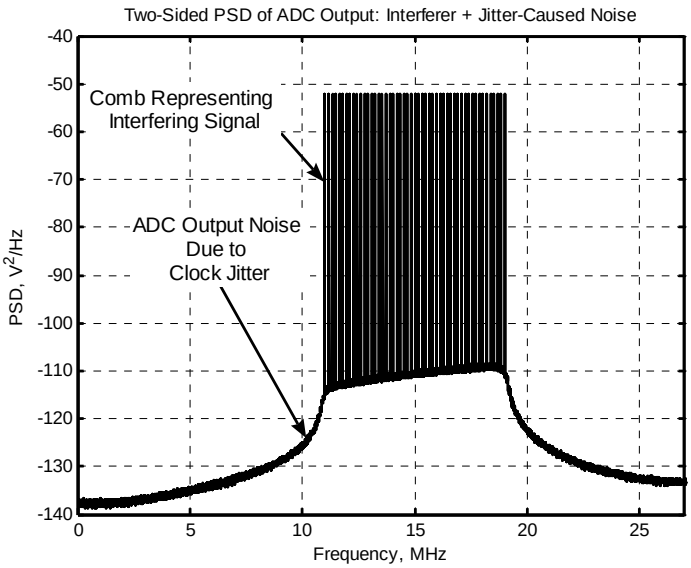

Figure 36 Reconstructed signal spectrum18 from ADC samples when the interfering signal is represented by a comb of equal-amplitude tones and the ADC clock-jitter is Lorentzian.[19]

12 Image Rejection

Image rejection in the presence of gain and phase imbalance between the *I* and *Q* channels is given by[20]

$$IR_{dB}(g,\theta) = 10\log_{10}\left[\frac{1+g^2+2g\cos(\theta)}{1+g^2-2g\cos(\theta)}\right] \tag{102}$$

where

$$g = 10^{0.1\Delta G_{dB}} \tag{103}$$

In the case where the phase imbalance is negligibly small, (102) reduces to

$$IR_{dB}(g) = 20\log_{10}\left[\left|\frac{1+g}{1-g}\right|\right] \tag{104}$$

The gain and phase imbalance can also be represented in terms of an error vector magnitude (EVM) value as[21]

$$EVM_{\%rms} = \sqrt{2-2\cos\left(\frac{\theta}{2}\right)+\left(\frac{\delta}{2}\right)^2} \quad \times 100\% \tag{105}$$

[18] Ibid.
[19] Figure 9-2 from [1].
[20] [1], equ. (5A.1)
[21] [1], equ. (5A.10).

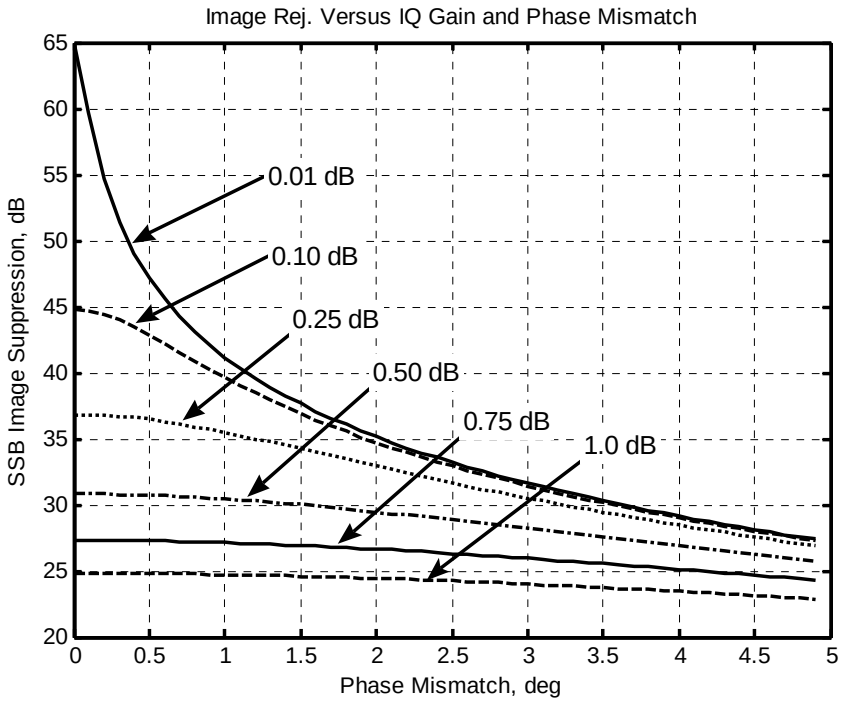

Figure 37 IQ SSB image rejection versus gain and phase mismatch.[22]

[22] [1], page 212. Computed in Book CD:\Ch5\u13149_iq_imbal_evm.m.

13 ADC Related SNR

When[23] an analog signal is sampled by a digitizer with finite quantization intervals, it can readily be shown that the achievable signal-to-quantization noise ratio (*SQNR*) is given by (e.g., Proakis, 108 page 37)

$$SQNR = 10\log_{10}\left(\frac{3}{2}2^{2N}\right) = 1.76 + 6.02N \text{ dB} \tag{106}$$

where *N* is the number of ADC quantization steps being used. The maximum *SNR* that a practical ADC can achieve is primarily limited by its analog noise performance, dynamic non-linearities (DNLs) in the conversion process and sampling-clock jitter. Equation (106) can be modified to include these factors as

$$SQNR = 1.76 - 10\log_{10}\left\{\left(\frac{2\sqrt{2}b_{rms}}{2^N}\right)^2 + \left(2\pi f_{in}\tau_{jitter}\right)^2 + \left(\frac{1+\varepsilon}{2^N}\right)^2\right\} \tag{107}$$

where

f_{in}	Analog input frequency, Hz
τ_{jitter}	ADC sampling clock aperture jitter, sec RMS
ε	Average DNL of the converter
b_{rms}	Equivalent RMS thermal noise in terms of ADC LSBs
N	Number of ADC bits

The SNR of the ADC can be converted to an equivalent noise figure as

$$NF_{ADC} = P_{fullscale} - SQNR - 10\log_{10}\left(\frac{f_s}{2}\right) + 174 \text{ dB} \tag{108}$$

where

$P_{fullscale}$	ADC's full-scale input power level
f_s	ADC sampling rate, Hz
NF_{ADC}	Equivalent noise figure of the ADC, dB

[23] Largely taken from [2] page 100.

14 Memoryless Bandpass Nonlinearities

Consider a memoryless polynomial based nonlinearity voltage function given by

$$x_{out} = \alpha_1 x + \alpha_3 x^3 \tag{109}$$

where the α's are constants that are determined by the nature of the voltage nonlinear transfer function. We will assume that the input signal x is a real-valued wide-sense stationary random process, and the output power spectral density (PSD) can therefore be computed by making use of the Weiner-Khintchine Theorem. The first step in computing the PSD is to compute the autocorrelation function for the output voltage x_{out}.

The autocorrelation function for the nonlinear portion $x_{nl} = \alpha_3 x^3$ is given by

$$R_{xnl}(\tau) = E\left\{x_{nl}(t)\, x_{nl}(t-\tau)\right\} \tag{110}$$

which can be expanded to give

$$R_{xnl} = E\left\{\alpha_3^2 x_{in}^3[t]\, x_{in}^3[t-\tau]\right\} = E\left\{\alpha_3^2 x^3 x_\tau^3\right\} \tag{111}$$

In this form, $x_\tau = x(t-\tau)$ for shorthand convenience. In order to proceed further, it is necessary to provide two identities that are true for Gaussian random variables n_1, n_2, etc.:

$$E\left\{n_1 n_2 n_3 n_4\right\} = \overline{n_1 n_2} \bullet \overline{n_3 n_4} + \overline{n_1 n_3} \bullet \overline{n_2 n_4} + \overline{n_1 n_4} \bullet \overline{n_2 n_3} \tag{112}$$

$$\begin{aligned} E\left\{n_1 n_2 n_3 n_4 n_5 n_6\right\} = {} & \overline{n_1 n_2}\left\{\overline{n_3 n_4} \bullet \overline{n_5 n_6} + \overline{n_3 n_5} \bullet \overline{n_4 n_6} + \overline{n_3 n_6} \bullet \overline{n_4 n_5}\right\} + \\ & \overline{n_1 n_3}\left\{\overline{n_2 n_4} \bullet \overline{n_5 n_6} + \overline{n_2 n_5} \bullet \overline{n_4 n_6} + \overline{n_2 n_6} \bullet \overline{n_4 n_5}\right\} + \\ & \overline{n_1 n_4}\left\{\overline{n_2 n_3} \bullet \overline{n_5 n_6} + \overline{n_2 n_5} \bullet \overline{n_3 n_6} + \overline{n_2 n_6} \bullet \overline{n_3 n_5}\right\} + \\ & \overline{n_1 n_5}\left\{\overline{n_2 n_3} \bullet \overline{n_4 n_6} + \overline{n_2 n_4} \bullet \overline{n_3 n_6} + \overline{n_2 n_6} \bullet \overline{n_3 n_4}\right\} + \\ & \overline{n_1 n_6}\left\{\overline{n_2 n_3} \bullet \overline{n_4 n_5} + \overline{n_2 n_4} \bullet \overline{n_3 n_5} + \overline{n_2 n_5} \bullet \overline{n_3 n_4}\right\} \end{aligned} \tag{113}$$

The over-bar in equations (112) and (113) represent statistical expectation (i.e., **E**(…)). Using these two identities along with the Weiner-Khintchine Theorem, the PSD of the output signal can be written as

$$S_{out}(f) = \beta_1 S(f - F_o) + \beta_3 S_3(f - F_o) \tag{114}$$

in which S(f) represents the power spectral density of the baseband modulation signal and

$$\beta_1 = \alpha_1^2 + \alpha_3^2 \frac{81}{32}\sigma_x^4$$
$$\beta_3 = \alpha_3^2 \frac{54}{32} \tag{115}$$

$$S_3(f) = S(f) \otimes S(f) \otimes S(f) \tag{116}$$

The symbol ⊗ in equation (116) represents convolution in the frequency domain. The spectrum $S_3(f)$ must also include the effects of any local oscillator phase noise as well (prior to the frequency convolution computation). It is not difficult to show that in the case of a rectangular S(f) baseband spectrum that

$$S_3(f) = \frac{\sigma_x^6}{8B^3}\begin{cases} 3B^2 - f^2 & if\ |f| \le B \\ \dfrac{(3B - |f|)^2}{2} & for\ B < |f| \le 3B \\ 0 & Otherwise \end{cases} \tag{117}$$

The result provided by (114) can be used to compute the power spectral densities at the nonlinearity output.

It is very worthwhile to point out that all but the α_1^2 term in β_1 represent intermodulation noise due to the nonlinearity. As a result, there is an intermodulation noise spectrum term that has the same PSD shape as the desired signal spectrum and this cannot generally be seen on a spectrum analyzer because it is overshadowed by the presence of the stronger desired signal components.

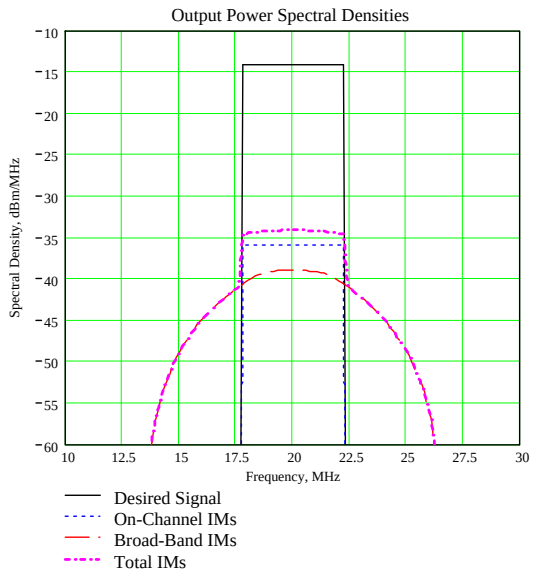

Figure 38 Example spectrum with total input power level 5 dB below the input 1 dB compression point. SNR at channel center is 19.96 dB.[24]

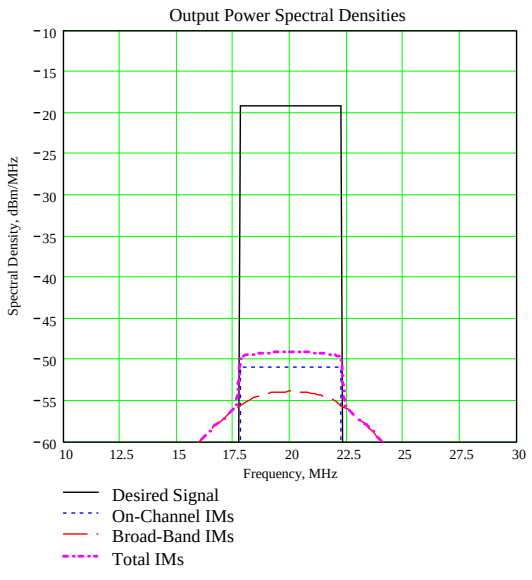

Figure 39 Example spectrum with total input power level 10 dB below the input 1 dB compression point. SNR at channel center is 29.96 dB.

[24] From U22599 IMs and OFDM SNR- van den Bos.mcd.

A popular model for an amplifier's memoryless nonlinear characteristics is the Rapp model which is given by[25]

$$g(v) = \frac{1}{\left(1 + |v|^{2n}\right)^{\frac{1}{2n}}} \tag{118}$$

with v representing the signal's complex-envelope magnitude and n is the single modeling parameter. Representative transfer functions are graphically shown for different values of n in Figure 40.

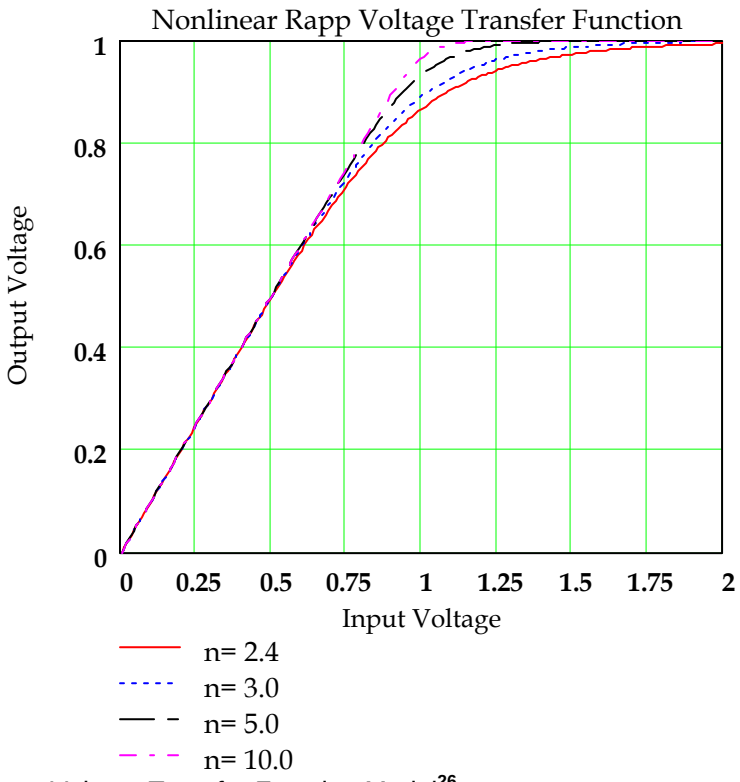

Figure 40 Rapp Nonlinear Voltage Transfer Function Model[26]

[25] C. Rapp, "Effects of HPA-Nonlinearity on a 4-DPSK/OFDM-Signal for a Digital Sound Broadcasting System", in Proceedings of the Second European Conference on Satellite Communications, Liege, Belgium, Oct. 22-24, 1991, pp. 179-184.

[26] From U11707

15 Appendix: Nonlinear IQ Expansions[27]

The expansions collected in Table 11 are very helpful when dealing with memoryless nonlinearities.

Table 11 On-Channel Intermodulation in Terms of I & Q

Order n, $s^n(t)$, for Surviving Terms	Terms
$\left[I\cos(\omega_o t)-Q\sin(\omega_o t)\right]^1 \Rightarrow$ $I_{NL}\cos(\omega_o t)-Q_{NL}\sin(\omega_o t)$	$I_{NL}=I$ $Q_{NL}=Q$
$\left[I\cos(\omega_o t)-Q\sin(\omega_o t)\right]^3 \Rightarrow$ $I_{NL}\cos(\omega_o t)-Q_{NL}\sin(\omega_o t)$	$I_{NL}=\frac{3}{4}\left[I^3+IQ^2\right]$ $Q_{NL}=\frac{3}{4}\left[Q^3+I^2Q\right]$
$\left[I\cos(\omega_o t)-Q\sin(\omega_o t)\right]^5 \Rightarrow$ $I_{NL}\cos(\omega_o t)-Q_{NL}\sin(\omega_o t)$	$I_{NL}=\frac{5}{8}I^5+\frac{5}{4}I^3Q^2+\frac{5}{8}IQ^4$ $Q_{NL}=\frac{5}{8}I^4Q+\frac{5}{4}I^2Q^3+\frac{5}{8}Q^5$
$\left[I\cos(\omega_o t)-Q\sin(\omega_o t)\right]^7 \Rightarrow$ $I_{NL}\cos(\omega_o t)-Q_{NL}\sin(\omega_o t)$	$I_{NL}=\frac{35}{64}I^7+\frac{105}{64}I^5Q^2+\frac{105}{64}I^3Q^4+\frac{35}{64}IQ^6$ $Q_{NL}=\frac{35}{64}I^6Q+\frac{105}{64}I^4Q^3+\frac{105}{64}I^2Q^5+\frac{35}{64}Q^7$
$\left[I\cos(\omega_o t)-Q\sin(\omega_o t)\right]^9 \Rightarrow$ $I_{NL}\cos(\omega_o t)-Q_{NL}\sin(\omega_o t)$	$I_{NL}=\frac{63}{128}I^9+\frac{252}{128}I^7Q^2+\frac{378}{128}I^5Q^4+\frac{252}{128}I^3Q^6+\frac{63}{128}IQ^8$ $Q_{NL}=\frac{63}{128}I^8Q+\frac{252}{128}I^6Q^3+\frac{378}{128}I^4Q^5+\frac{252}{128}I^2Q^7+\frac{63}{128}Q^9$
$\left[I\cos(\omega_o t)-Q\sin(\omega_o t)\right]^{11} \Rightarrow$ $I_{NL}\cos(\omega_o t)-Q_{NL}\sin(\omega_o t)$	$I_{NL}=\frac{231}{512}I^{11}+\frac{1155}{512}I^9Q^2+\frac{2310}{512}I^7Q^4+\frac{2310}{512}I^5Q^6+\frac{1155}{512}I^3Q^8+\frac{231}{512}IQ^{10}$ $Q_{NL}=\frac{231}{512}I^{10}Q+\frac{1155}{512}I^8Q^3+\frac{2310}{512}I^6Q^5+\frac{2310}{512}I^4Q^7+\frac{1155}{512}I^2Q^9+\frac{231}{512}Q^{11}$

[27] From U11706.

16 Appendix: Amplitude Distribution of OFDM Signals[28]

Strictly speaking, any OFDM signal appears as a cyclostationary random process to a phase-synchronized receiver. Without synchronization however (as in the case of an interfering OFDM adjacent channel signal), the cyclostationary process becomes a wide-sense stationary process.

The OFDM complex baseband signal for N subcarriers can be written as

$$x(t) = \sum_{n=1}^{N} a_n \cos(\omega_n t) + b_n \sin(\omega_n t) \tag{119}$$

Here, the a_n and b_n are the in-phase and quadrature-phase modulating symbols for each OFDM subcarrier. From the Central Limit Theorem, it follows that for large values of N, the real and imaginary values of x(t) become Gaussian distributed. The amplitude of the OFDM signal therefore has a Rayleigh distribution with zero mean and a variance of *N* times the variance of one complex sinusoid. The power distribution becomes a central chi-square distribution with 2 degrees of freedom and zero mean, with the cumulative distribution given by

$$F(z) = \int_0^z \frac{e^{-\frac{u^2}{2\sigma^2}}}{2\sigma^2} du = 1 - e^{-\frac{z}{2\sigma^2}} \tag{120}$$

In order to derive the cumulative distribution function of the peak power per OFDM symbol, we will first assume that the time samples z are mutually uncorrelated. This is only true however, for non-oversampled situations (samples taken at the Nyquist rate). The cumulative distribution under this assumption is given by [12]

$$G_z(N, z) = \left[1 - e^{-\frac{z}{2\sigma^2}}\right]^N \tag{121}$$

In the case of real continuous time in which oversampling is present (which would violate the sample independence that was exploited in deriving (121)), it has been shown [12] that a very accurate cumulative distribution for $N \geq 64$ is given by

$$G_z(N, z) = \left[1 - e^{-\frac{z}{2\sigma^2}}\right]^{\alpha N} \tag{122}$$

in which $\alpha = 2.8$.

[28] From U11706.

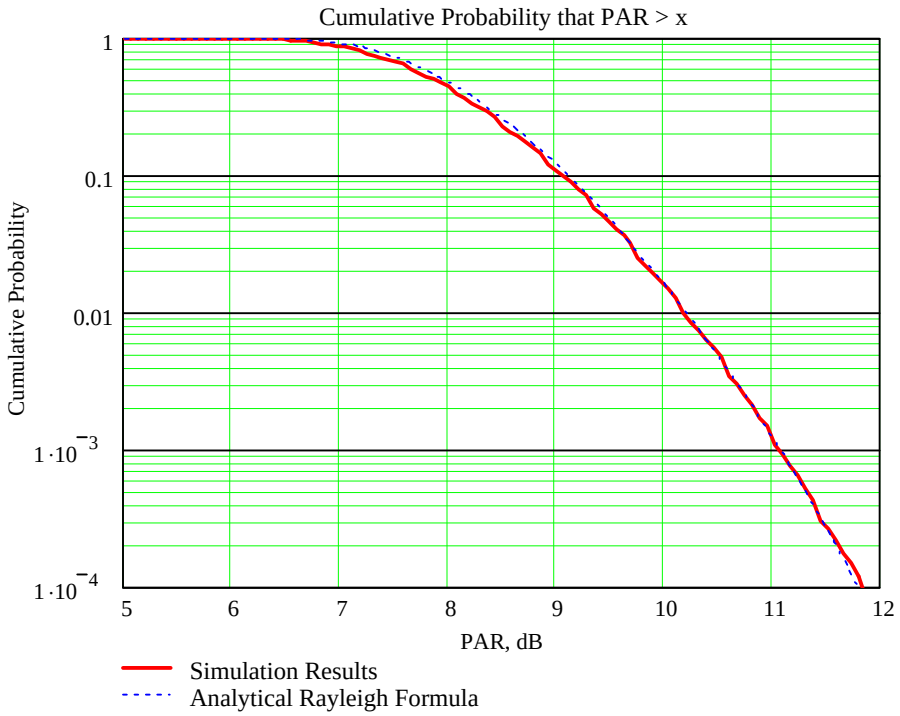

Figure 41 PAPR Simulation Results[29] for 64-QAM, 128 Tones, 250,000 OFDM Symbols, Over-Sampling Rate= 8

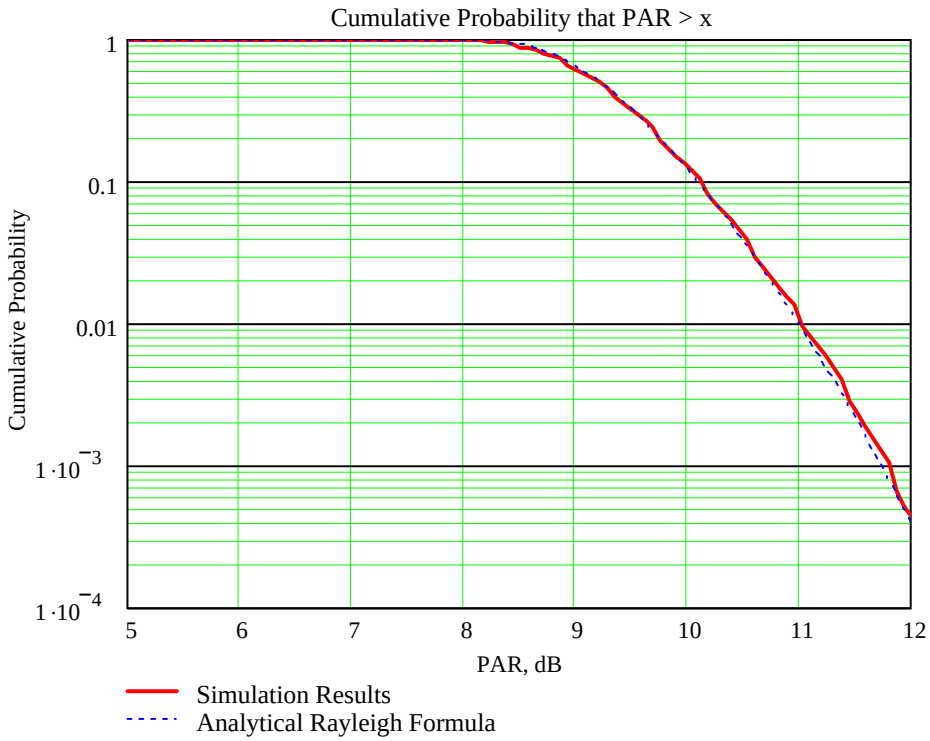

Figure 42 PAPR Simulation Results for 64-QAM, 1024 Tones, 250,000 OFDM Symbols, Over-Sampling Rate= 8

[29] From U11718

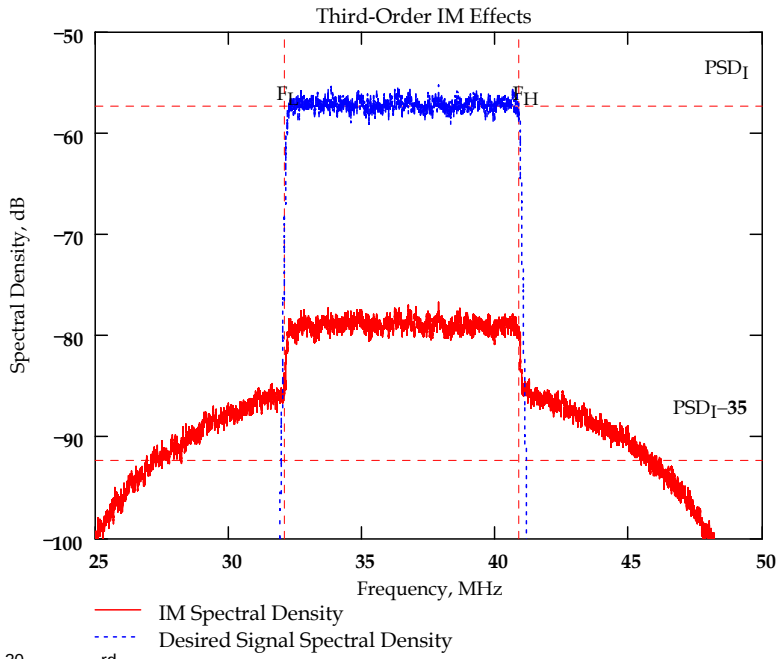

Figure 43 Spectrum[30] with 3rd-Order Nonlinearity, Back-Off From P_{1dB}= 5 dB. Average On-Channel SNR= 21.7 dB; Adjacent Channel IM Level= -28.7 dBc

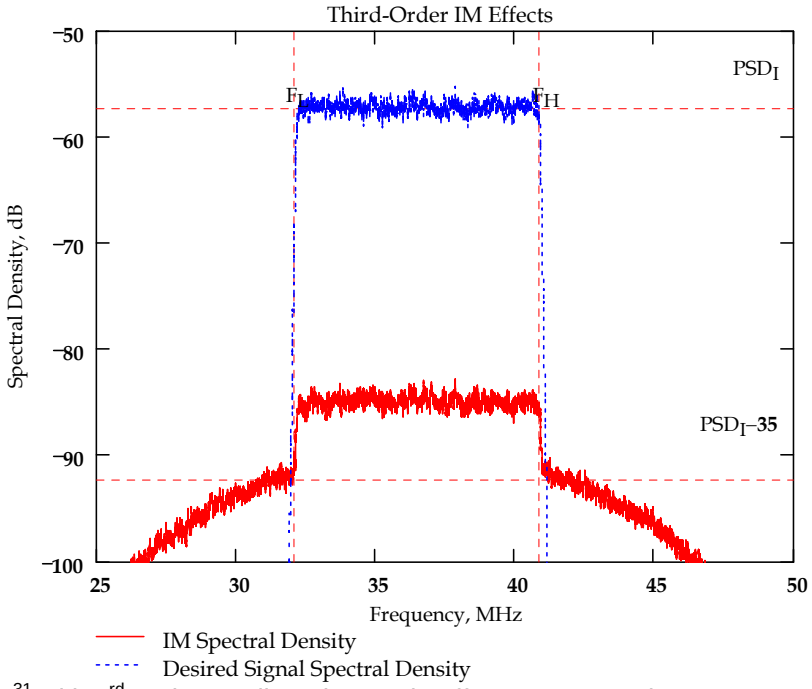

Figure 44 Spectrum[31] with 3rd-Order Nonlinearity, Back-Off From P_{1dB}= 8 dB. Average On-Channel SNR= 27.7 dB; Adjacent Channel IM Level= -34.7 dBc

[30] From U11707. Modulation bandwidth= 8.75 MHz. OFDM modulation modeled as a rectangular spectrum of Gaussian noise.
[31] From U11707. Modulation bandwidth= 8.75 MHz. OFDM modulation modeled as a rectangular spectrum of Gaussian noise.

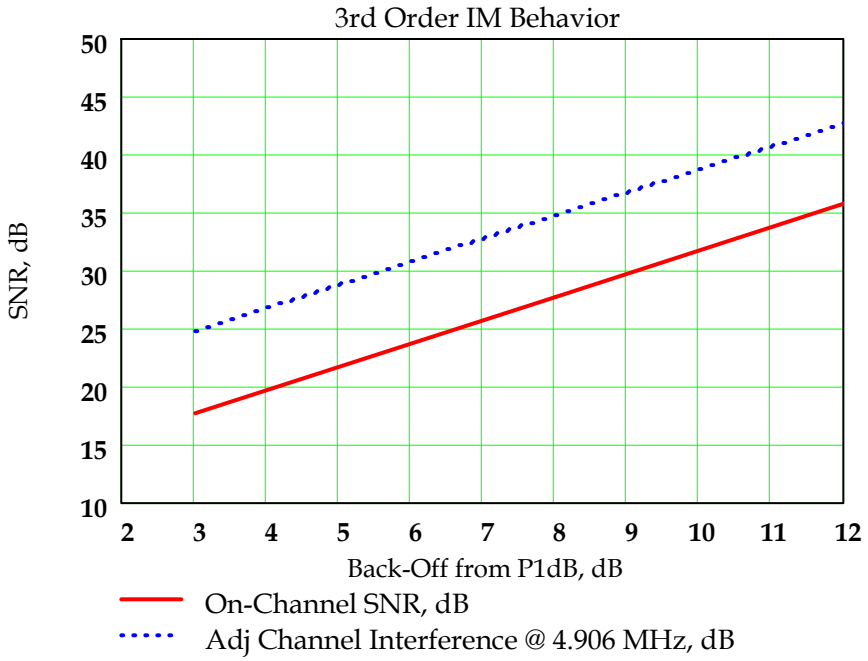

Figure 45 Simulation Predictions[32] for On-Channel SNR and Adjacent Channel Leakage Versus P_{1dB}

[32] From U11707; Modulation BW= 8.75 MHz, Channel Spacing= 10 MHz. OFDM modulation modeled as a rectangular spectrum of Gaussian noise.

16.1 Results with Rapp Model (n=2.4)[33]

IM spectrum results using the Rapp model are shown for several back-off levels in the following figures.

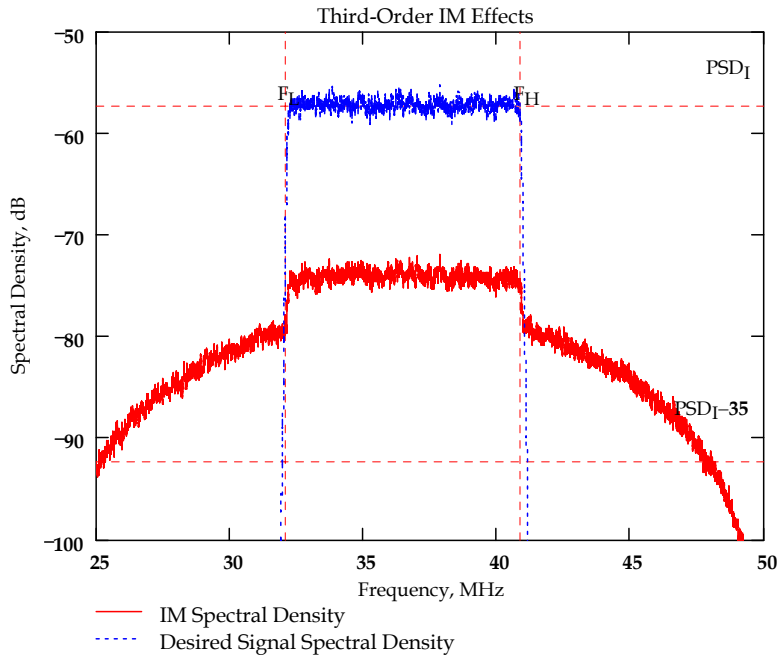

Figure 46 Spectrum[34] with Rapp Nonlinearity (n=2.4), Back-Off From P_{1dB}= 3 dB. Average On-Channel SNR= 16.8 dB; Adjacent Channel IM Level= -22.6 dBc

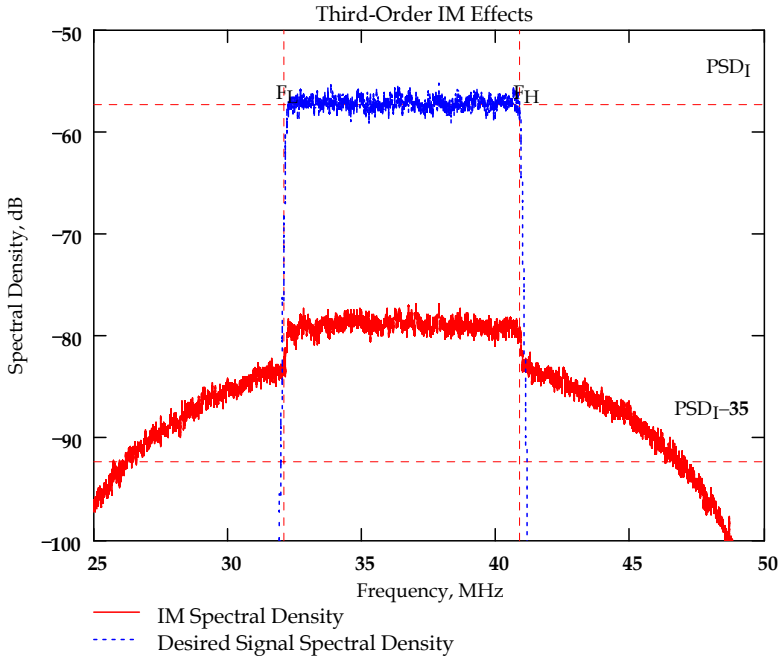

Figure 47 Spectrum[35] with Rapp Nonlinearity (n=2.4), Back-Off From P_{1dB}= 5 dB. Average On-Channel SNR= 21.6 dB; Adjacent Channel IM Level= -26.3 dBc

[33] From U11706.
[34] From U11707. Modulation bandwidth= 8.75 MHz

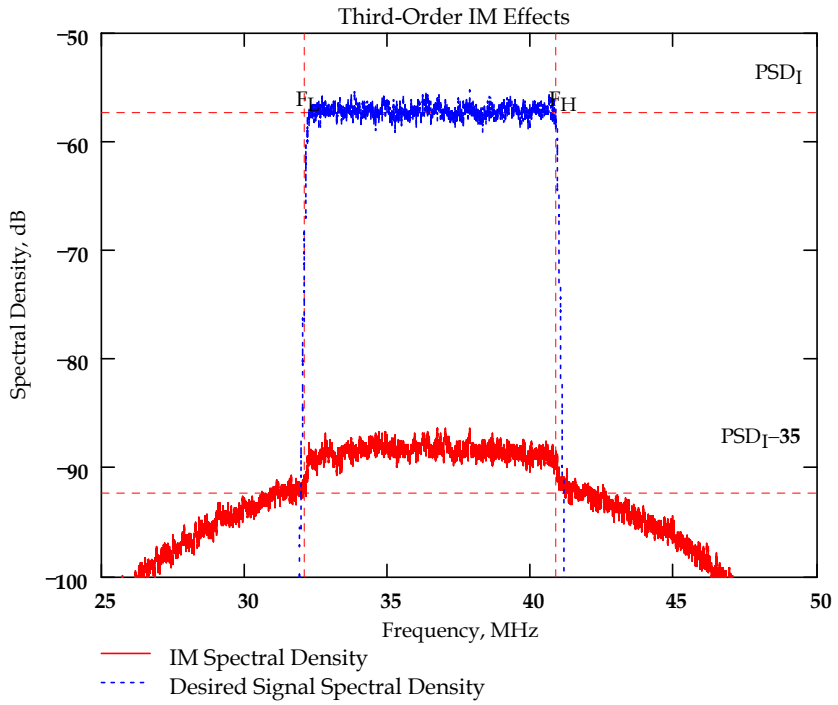

Figure 48 Spectrum[36] with Rapp Nonlinearity (n=2.4), Back-Off From P_{1dB}= 8 dB. Average On-Channel SNR= 30.8 dB; Adjacent Channel IM Level= -34.5 dBc

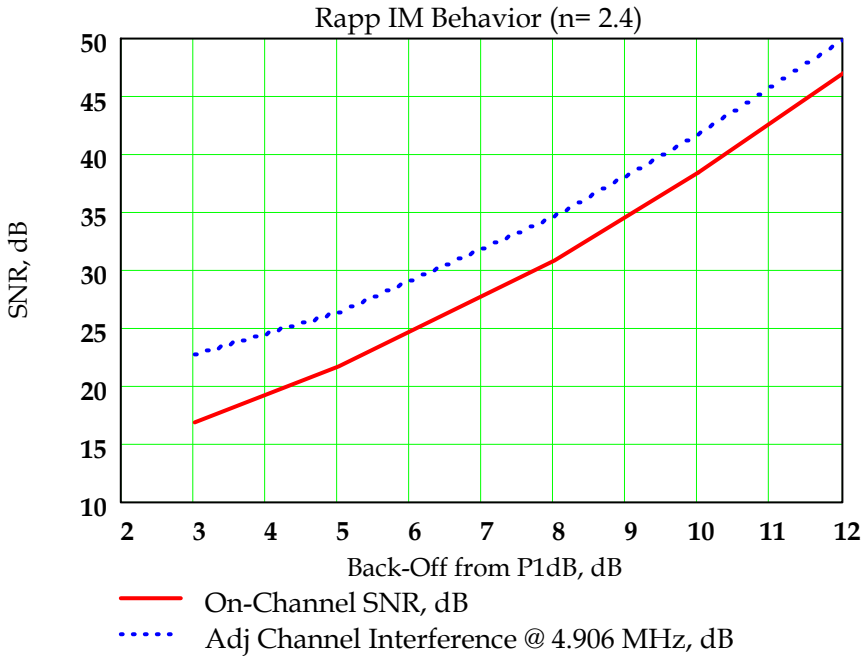

Figure 49 IM Behavior[37] with Rapp Model (n=2.4) for Unsynchronized Receiver Case

[35] From U11707. Modulation bandwidth= 8.75 MHz. OFDM modulation modeled as a rectangular spectrum of Gaussian noise.
[36] From U11707. Modulation bandwidth= 8.75 MHz. OFDM modulation modeled as a rectangular spectrum of Gaussian noise.

17 Standards

17.1 MIL-STD-188-243: AM / FM Sensitivity

Measured using a source impedance of 50Ω, and 1 kHz audio tone.[38]

Mode	Rx Input Power Level, dBm	Rx Input Voltage, μV RMS	Modulation Index / Peak Deviation	–6 dB BW, –60 dB BW, kHz	Output Audio SNR, dB
AM:					
Narrowband	–103.5	1.5	30%	24 | 50	10
Wideband	–101	2.0	30%	70 | 140	10
FM:					
Narrowband	–103.5	1.5	5 kHz	24 | 50	10
Wideband	–101	2.0	20 kHz	70 | 140	10
PRC-117(F)[39]					
AM	–110		70%		10
FM	–116				10
Harris Falcon III[40]					
AM	–110		70%		12
FM	–116				12
Rockwell ARC-210[41]					
AM	–103				
FM	–108				

[37] U11707
[38] CSEL00182 MIL-STD-188-243.pdf.
[39] U22796 HAVEQUICK AN_PRC117F.pdf.
[40] U22795 Harris Falcon Manpack.pdf.
[41] U22799 ARC-210 Gen5 brochure.pdf.

18 References

1. J.A. Crawford, *Advanced Phase-Lock Techniques*, Artech House, 2008.
2. Nigel C. Davies, “Digital Radio and Its Application in the HF (2–30 MHz) Band,” Dissertation, May 2004, U22156.
3. Thomas C. Steidel, “Programs Simplify Systems Analysis,” *Microwaves & RF*, Jan. 1985.
4. Robert E. Snyder, “Use Filter Models to Analyze Receiver IM,” *Microwaves*, Nov. 1978.
5. Walid Y. Ali-Ahmad, “Effective IM2 Estimation for Two-Tone and WCDMA Modulated Blockers in Zero-IF,” *rf design*, April 2004, CSEL00201.
6. Tri T. Ha, *Solid-State Microwave Amplifier Design*, John Wiley & Sons, 1981.
7. Jacques C. Rudell, Jeffrey A. Weldon, et al., “An Integrated GSM/DECT Receiver: Design Specifications,” UCB Electronics Research Laboratory Memorandum, Memo #: UCB/ERL M97/82, Revised 28 April 1998, U22177.
8. Analog Devices by Walt Kester, “Noise Power Ratio (NPR)– A 65–Year Old Telephone System Specification Finds New Life in Modern Wireless Communications,” MT-005 Tutorial, U18708.
9. AM1 LLC, Version 0.67, U21680.
10. _____,” Version 3.0, 24 Sept. 2014, U21118.
11. _____, “Spectrum Occupancy Effects with OFDM-Type Signals Due to Phase Noise and Transmitter Nonlinearities,” 8 April 2005, U11706.
12. Van Nee, R., de Wild, A., “Reducing the Peak-to-Average Power Ratio of OFDM”, IEEE VTC 1998 (M12209)